Olai Stensland Lillevold

Thermal design of jointed precast concrete energy piles

Semi-empirical g-functions for driven square piles and the influence of surface boundary condition

Masteroppgave

NTNU
Kunnskap for en bedre verden

Olai Stensland Lillevold

Thermal design of jointed precast concrete energy piles

Semi-empirical g-functions for driven square piles
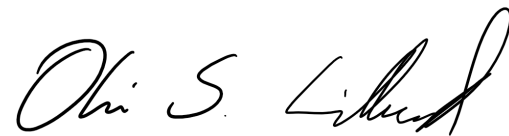and the influence of surface boundary condition

**NTNU**

Kunnskap for en bedre verden

Preface

One year ago, the subject of ground source energy was virtually an utterly undiscovered terrain to me. It has nonetheless been an pleasure to start the expedition into this underground world of renewable energy sources.

This thesis is the ending project of the MSc in Civil and Environmental Engineering with Geotechnical Engineering as main profile. The scope of the project is 30 ECTS in the subject TBA4900. The project was carried out during the winter 21/22.

Trondheim, 2022-02-10

Olai Stensland Lillevold
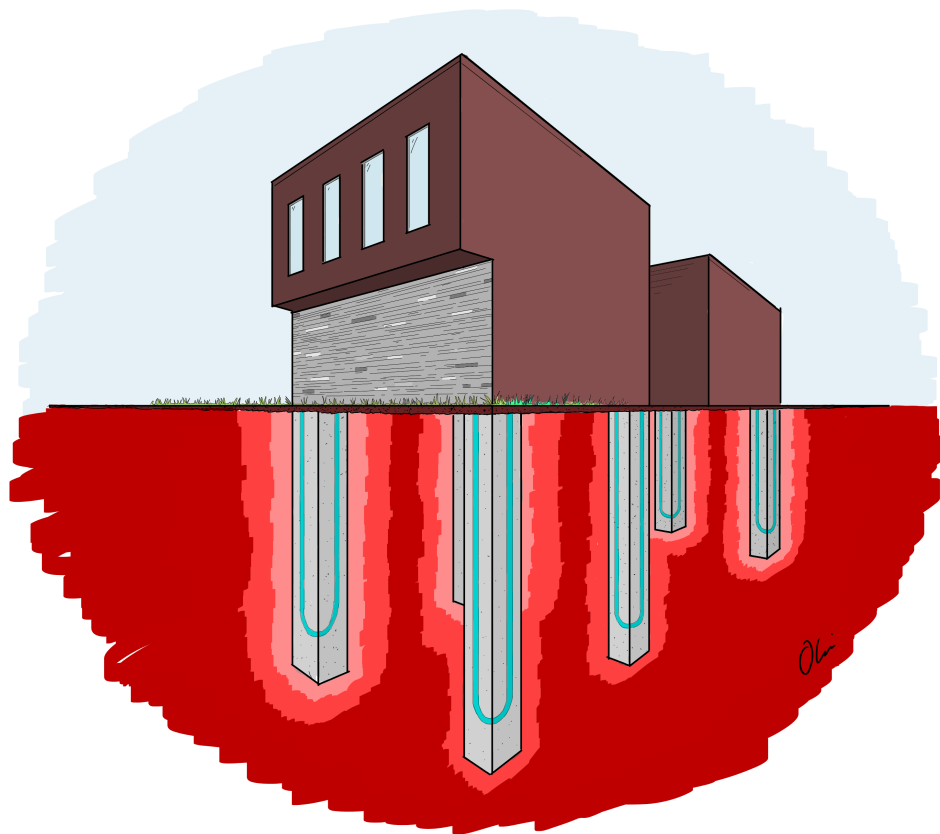
Acknowledgment

First of all, I want to thank Professor Rao Martand Singh for guidance throughout the last year. I have found the weekly meetings enjoyable, and your insight and enthusiasm in the subject have been valuable and inspiring. I also want to express my fullest gratitude for the help of Ph.D. Candidate Habibollah Sadeghi. Your contribution has been crucial, sharing your knowledge and always being available to help with a matter. It has been a pleasure working with you both.

Furthermore, I want to thank my friend, Simen Aamodt. I admire your virtuosity, and I am truly grateful for your taking the time to share some of your expertise in computational modeling. I also want to thank my parents, brother and friends for always being supportive, my mate Henry for proofreading, and especially Tonje, who always back me up, and exceptionally the last few weeks.

<div align="right">Olai S.L</div>

Abstract

Energy geostructures, extracting and storing heat in the ground, are utilized as heat or sink to constructions. They exist as different constructions such as energy tunnels, energy walls, and energy piles, which are studied in this thesis. The energy geostructures provide cost-minimizing and efficient renewable energy.

In this thesis, a validated method to obtain semi-empirical dimensionless temperature response functions, g-functions, for driven square energy piles, has been adopted. A 3D FEM model was made and validated with field data, which comprised an energy pile of concrete with the pipes embedded and the ambient soil. Some assumptions made were isotropic and homogeneous material of the concrete, soil and pipes, and pure conduction in the concrete and soil. G-functions are utilized for the thermal design of ground source heat pumps. G-functions for different pile widths, lengths, and pipe configurations, have been produced and are presented in this thesis. Aspect ratios between 30 and 130 have been studied for energy piles, which is higher than previous work.

Concrete response functions have been produced, accounting for the transient behavior of the piles, which yields more accurate design fluid temperatures by considering the development of pile resistance in daily fluctuations of thermal load.

The ground level surface boundary condition has been studied. The 3D FEM model of this thesis was made with adiabatic insulation and compared with another model with a constant temperature boundary condition. The different models had similar values for Fo < 10, which would correspond to about 100 hours. After this, however, was there a large difference in the long term. Adiabatic insulation yields higher temperature response, and the difference was especially large with shorter piles. The g-functions of this paper can be utilized for interpretation of thermal response testing and short-term temperature calculations and can also give conservative estimates for long-term thermal design.

Sammendrag

Energy geostructures - geoenergi-konstruksjoner - er en type grunnvarmepumpe der konstruksjoner i bakken blir utnyttet til å hente ut eller lagre termisk energi i bakken. Energikonstruksjonene finnes i dag som energivegger, energituneller, eller energipeler, som er i fokus i denne oppgaven. Energikonstruksjonene er en gunstig tilnærming til oppvarming og nedkjøling av bygg da det benyttes konstruksjoner som allerede har en funksjon, og de stabile temperaturene i grunnen gir et godt grunnlag for effektiv, fornybar energi.

I denne oppgaven er det tatt i bruk en verifisert metode for å produsere semi-empririske dimensjonsløse temperaturrespons-funksjoner, g-funksjoner, for energipeler. En 3D FEM model ble laget og validert med feltdata, bestående av en betongpele, kollektorslangene inne i pelefundamentet, og den omkringliggende grunnen. Antagelser som ble gjort var isotropisk og homogene betong, kollektor, og jord-materialer med kun varmeledning som varmeover-føringsmekanisme. G-funksjoner kan brukes ved dimensjonering av termiske systemer i bakken. I denne oppgaven har blitt produsert g-funksjoner for forskjellige peledimensjoner, lengder, og anretning av kollektorslanger.

Bredde-lengde strørrelsesforhold mellom 30 og 130 har blitt undersøkt, noe som er høyere enn tidligere studert for energipeler. I tillegg har det blitt produsert responsfunksjoner for utviklingen av den termiske resistansen til betongen. Ved hjelp av disse responsfunksjonene av betongen kan man ta den transiente responsen til betongen, med daglige svingninger i termisk behov, med i betraktningen ved termisk dimensjonering av energipeler.

Randbetingelsene for modellens overflate som tilsvarer bakkeplanet ble i tillegg undersøkt. Modellen i denne oppgaven hadde en adiabatisk isolert overflate, og ble sammenlignet med lignende 3D FEM modell med konstant temperatur som randbetingelse. Modellene viste samsvarende verdier etter kort tid med Fo < 10, tilsvarende omtrent 100 timer, men ved lengre tid ga randbetingelsene store utslag. Adiabatisk isolering ga høyere temperaturrespons, og spesielt kortere peler ble påvirket mye. G-funksjonen kan dermed brukes for kortere estimering av temperaturen til varmebæreren og implementering i termisk responstesting, og kan gi konservative estimater for termisk dimensjonering ved langtidssimulering.

Nomenclature

Symbols

α_s Soil thermal diffusity $[m^2/s]$

λ_c Concrete conductivity [W/(mK)]

λ_g Soil conductivity [W/(mK)]

λ_{pipe} Pipe conductivity $[W/(mK)]$

ϕ Normalised temperature change

c_p Specific heat capacity $[MJ/(m^3 * K)]$

Fo Fourier number: Normalised time

G_c Concrete g-function

G_g Ground g-function

L_a Thermal active length of piles

q Heat transfer rate per meter active pile length [W/m]

R_c Concrete thermal resistance [m*K/W]

R_{pipe} Pipe thermal resistance [m*K/W]

$S_c v$ Volumetric heat capacity $[MJ/(kg * K)]$

T_0 Undisturbed soil temperature [°C]

T_b Pile wall temperature [°C]

T_f Heat carrier fluid temperature [°C]

T_p Pipe outer wall temperature [°C]

Abbreviations

AR   Aspect ratio

FEM   Finite element method

GEP   Geothermal energy pile

GHE   Ground heat exchanger

GSHP   Ground source heat pump

TRT   Thermal response test

Contents

Chapter 1

Introduction

Energy geostructures are used as the primary unit of a type of geothermal ground source heat pump (GSHP) system relying on the structures underneath ground level. They are used to extract thermal energy for heating and cooling of constructions. These energy geostructures exist in different shapes as energy piles, walls, and tunnels. These multi-functional structures take a holistic approach to heating and cooling of constructions, and they contribute as an environmental and cost-minimizing technology [1] [2]. This novel technology can meet some of the challenges that other GSHPs face. For borehole heat exchangers, the main challenges are increased drilling cost in relation to thick sedimentary deposits, space issues in densely populated areas, and high initial cost, as discussed by Ramstad (2011) [3].

Over the last two decades, there has been an increased awareness of the benefits of using geothermal energy and a significant increase in GSHP systems. From 2005 to 2010, worldwide direct geothermal energy use doubled and then nearly tripled from 2010 with about 200 000 TJ/year to almost 600 000 TJ/year in 2020 [4], where the 2020 numbers give yearly energy savings of 81 tonnes equivalent oil.

In the cold climate of Norway, as much as one-third of the total energy consumption is going to the heating and cooling of buildings [5], as shown in figure 1.1. At the same time, Ramstad (2011) [3] estimated that GSHP systems could cover the entire building heating and cooling demand in Norway. This describes the enormous potential of this energy source in Norway and other similar countries. Energy geostructures as energy piles have been implemented as a source of energy in many places worldwide since the beginning in Austria in the 1980s[1]. However, the technology has not yet been introduced in Norway.

Nonetheless, there is a large interest and knowledge in GSHPs. Several projects have already been initiated investigating energy geostructures under Norwegian conditions. The literature on energy geostructures stresses the need for accurate designing methods and increased knowledge in this area. Designed and installed the right way, GEPs can save energy, decrease CO_2 emissions, decrease pollution, and be economically beneficial even for smaller residential houses [6] (appendix C). For more information about the energy consumption, cost, and potential of energy piles in Norway, see the attached specialization project report in appendix C.
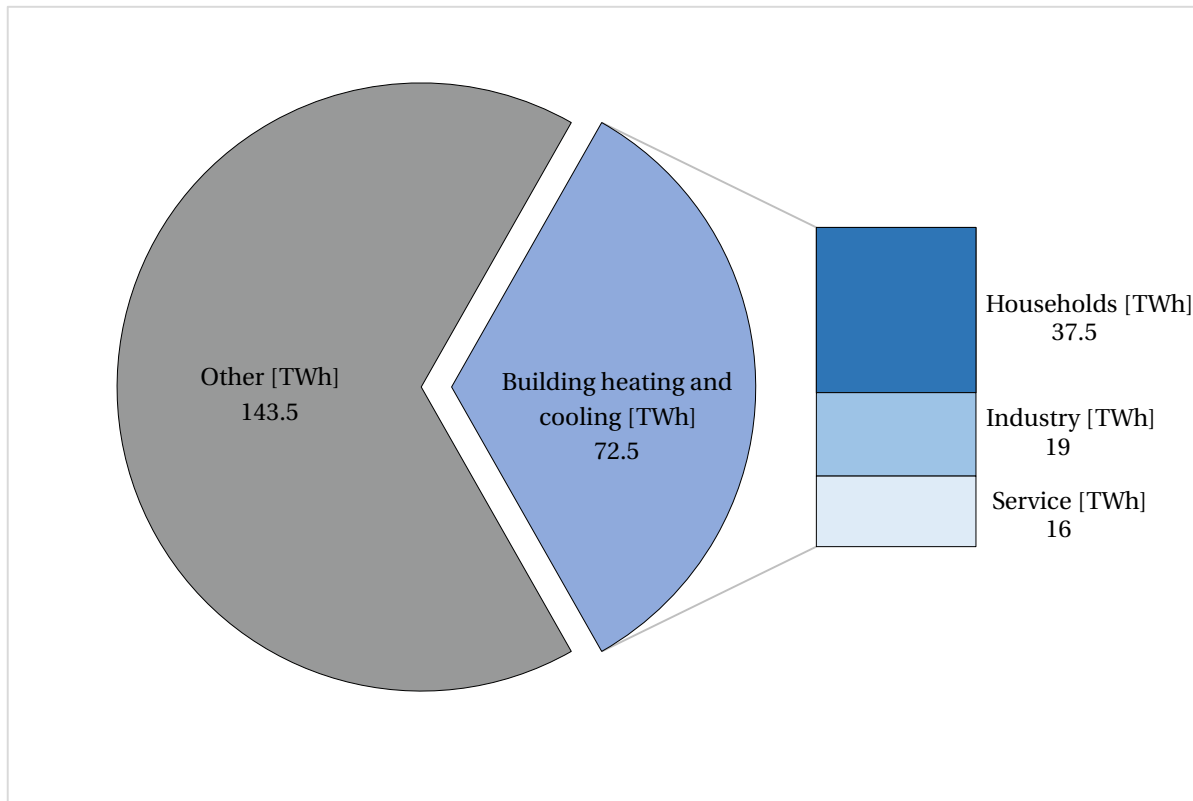
1

Figure 1.1: The share of building heating and cooling energy consumption of the total energy consumption in Norway (2018) and the breakdown of the use in the different sectors. Modified from source [5]

.

Thesis problem formulation

This thesis focuses on the thermal design of geothermal energy piles with specifically jointed quadratic driven precast concrete energy piles and the surface boundary condition for developing semi-empirical g-functions.

The work of this thesis is mainly based on the work of Loverigde (2012) [7], Loveridge & Powrie (2013) [8] and Alberdi-Pagola et al. (2019) [9]. Loverigde and Powrie (2013) proposed a method to obtain single energy pile g-functions and multiple energy pile g-functions by introducing a concrete G-function term in the calculation of GEP fluid temperature [8]. The g-functions were limited to upper and lower bound g-functions for piles with a circular cross-section. Alberdi-Pagola et al. [9] adopted the methods to energy piles with a square cross-section and the U-and W-shaped pipe configurations with lengths less than 15 meters.

The transient behavior of the pile concrete is necessary to consider in the thermal design. The concrete g-functions which is presented in chapter 2.5 was therefore introduced by Loveridge (2012) [7]

Loverigde and Powrie (2013) [8] and Alberdi-Pagola et al. (2019) [9] are looking at an aspect ratio (AR) from 15 to 53. With a diameter of 350 mm, the ARs would reflect a pile length of about 7 to 23 meters. Piles can be connected and elongated by jointing pile segments of 15 meters [10] and it is therefore a necessity to look at larger AR . In this thesis, the well-described method of obtaining g-functions in Alberdi-Pagola et al. (2018) [11] and

(2019) [9] is adopted and applied to piles with a square cross-section and both *W-* and *partly W-shaped* pipes with a larger aspect ratio (AR). Piles in Norway comes in the pile width of 270, 350 and 450 mm, and these pile widths are therefore studied. Furthermore is the surface boundary condition and the effect on the g-function investigated and presented.

A theoretical background for thermal design of energy piles is presented in chapter 2. This is followed by the FEM method, model and assumptions in chapter 3.2, results in chapter 4 followed by discussion and conclusions in chapter 5 and 6.

Chapter 2

Background

Geothermal energy comes from different sources [12]. At shallow depths under the ground surface level, stored solar radiation dominates the thermal energy present in the soil. This is the most relevant source regarding energy geostructures. For boreholes that go deeper, there is a temperature gradient where there is an increased heat flux from radioactive decay and the heat flux from the earth's hot interior. This chapter will go through the basics of heat transfer and soil temperatures at shallow depths in relation to the thermal design of energy piles.

2.1   Heat transfer in soil

Soil is a composite material composed of water, air, organic material, and mineralogical grains. The heat transfer mechanisms in the soil are complex and dependent on the soil properties, and conditions such as the particle sizes, the degree of saturation, and the temperature level [13]. Heat can be transferred in the soil through radiation, conduction, free or forced convection, and the effect of latent heat of phase change.

Electromagnetic radiation is present in air-filled pores in the soil. It is, however, usually negligible when looking at heat transfer through solid or fluid, and the contribution is less than 1% for sand and even less for finer-grained soils such as clay [14].

The effect of latent heat is in conjunction with thermal analysis of energy geostructures usually also considered negligible [15]. With that said, latent heat of vaporization can be noteworthy in fine-grained partially saturated soils, and the effect of latent heat of fusion can be important in the cold zones with permafrost [16] [17]. The latter is discussed further in 2.2.1

The effect of forced or free convection can be significant in highly permeable coarse-grained soils with groundwater flow present in the soil [18]. For low groundwater flow velocities or for soil with low permeability, the effect of convection can be regarded as negligible [15]. For the design of GEPs, any possible convection will contribute to an increased effective thermal conductivity.

Conduction is then the dominating heat transfer mechanism in the soil. One can see from figure 2.1 the complexity of the soil with the change of heat transfer mechanisms as a function of particle size and degree of saturation.

Despite the complexity of the heat transfer in soil, it is often been regarded as a pure thermal conduction process in thermal analysis [17]. Figure 2.1 was displayed to illustrate the limitations of the simplification of just taking conduction into account in mathematical models.
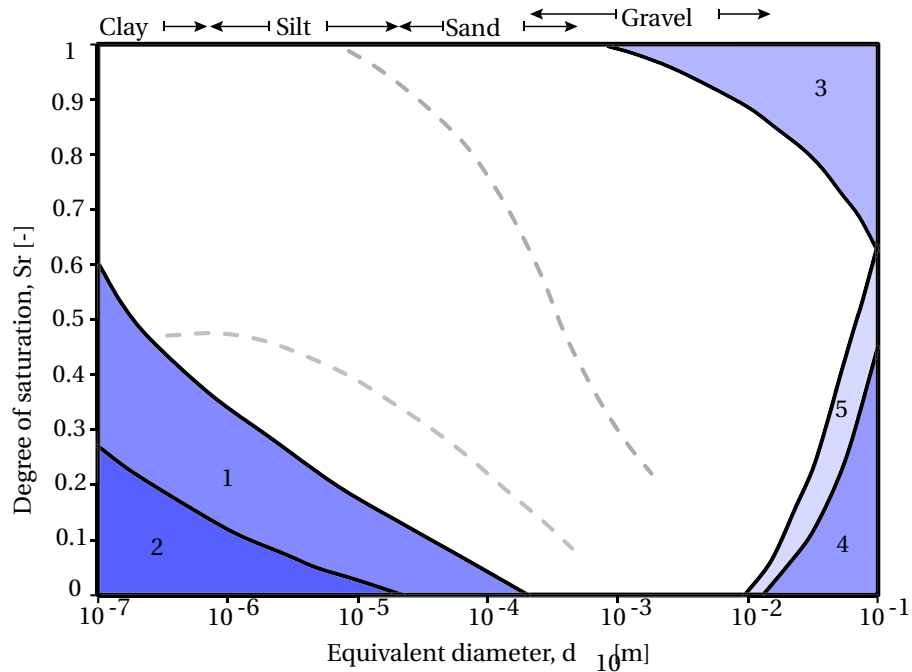
Figure 2.1: Modified from Johansen (1975) [17]. The grey lines show expected limits of saturation level in the base materials, sands and gravels in a road structure, and the numbers are referring to the heat transfer mechanisms:

1. Temperature dependent moisture migration

2. Moisture dependent vapour diffusion

3. Convective heat transfer in air

4. Convective heat transfer in water

5. Radiation of heat in voids

However, in the making of semi-empirical g-functions, only taking the conduction into account is reasonable, and this is the basis of the simulations done in the present work. Heat rate in an isotropic and homogeneous medium through conduction is expressed by Fourier's law [15] and presented in eguation 2.1

$$\dot{q} = \frac{\dot{Q}}{A} = -\lambda \nabla T \tag{2.1}$$

Where $\dot{q}$ is heat transfer rate, $\dot{Q}$ is the heat transfer flow, λ is the conductivity of the material with the cross-section area A. ∇ is the del-operator of the temperature field T. For the heat transfer analysis with only conduction considered, the conservation of energy is given by Fourier heat conduction equation with assumed constant heat conduction for a given volume [15], as presented in equation 2.1

$$\lambda \nabla^2 T + \dot{q} = \rho c_p \frac{\partial T}{\partial t} \tag{2.2}$$

The first term is connected to the rate of energy through the boundaries of the volume, $\dot{q}$ is the rate of the heat generated inside the volume, and the right side term is the amount of heat stored in the volume. The Laplace, ∇^2, expressed through cartesian coordinates, is:

$$\nabla^2 T = \frac{\partial^2 T}{\partial x^2} + \frac{\partial^2 T}{\partial y^2} + \frac{\partial^2 T}{\partial z^2}$$

2.1.1 Thermal conductivity

The thermal conductivity of soil is dependent on the temperature, volumetric composition considered as density and moisture content, the conductivity of the minerals, and the microgeometrical conditions [19] [17]. The different types of soils have a large variation of the thermal properties as shown in table 2.1. The density of the soil types varies from 1800 to 2300 kg/m^3 [20] in the field.

Table 2.1: Thermal conductivity and volumetric heat capacity for different soil types, concrete, and water from: Johansen (1976) [13], Sundberg (1991) [21], German standard VDI 4640 [20] with the recommended values of the standard in parentheses.

Material	Source	Thermal conductivity $[W/(mK)]$			Heat capacity $[MJ/(m^3 K)]$
		Dry	Saturated	Frozen	
Clay	*Johansen (1976)*		0.9-1.4	1.6-2.4	3.0-3.25
	Sundberg (1991)		0.85-1.5		2.9-3.6
	VDI 4640 (2010)	0.4-1.0 (0.5)	1.1-3.1 (1.8)		2.0-2.8
	VDI 4640 (2010)		1.8		2.0-2.8
Silt	*Johansen (1976)*		1.0-1.7	1.7-2.8	2.4-3.15
	Sundberg (1991)		1.2-2.4		2.4-3.3
	VDI 4640 (2010)	0.4-1.0	0.9-2.3		1.6-3.4
	VDI 4640 (2010)		1.8		2.0-2.8
	VDI 4640 (2010)	0.4-1.0 (0.5)	1.1-3.1 (1.8)		2.0-2.8
Sand	*Johansen (1976)*		1.1-2.2	0.8-1.8	1.8-1.9
	Sundberg (1991)		0.6-2.6		1.2-3.2
	VDI 4640 (2010)	0.3-0.9	2.0-3.0 (2.4)		2.2-2.8
	VDI 4640 (2010)		2.4		1.6-2.8
Gravel	*Johansen (1976)*		1.0-2.0	0.7-1.8	1.6
	Sundberg (1991)		0.6-2.5		1.3-3.0
	VDI 4640 (2010)	0.4-0.9 (0.4)	1.6-2.5 (1.8)		2.2-2.6
	VDI 4640 (2010)		1.8		2.2-2.6
Peat	*VDI 4640 (2010)*		0.2-0.7 (0.4)		0.5-3.8
Water	*Johansen (1976)*		0.582		4.192
Ice	*Johansen (1976)*		2.25		2.04
Concrete	*VDI 4640 (2010)*		0.9-2.0		1.8-2.0

When it comes to mineralogy, the thermal conductivity depends mainly on the amount of quartz in the soil. Quartz has a high thermal conductivity at around 7 W/mK, whereas other rock typically have values of 1-3 W/mK [12]. The soil conductivity increases with increased saturation and increased dry density.

Since thermal conductivity is dependent on the microgeometrical conditions, it is in most cases necessary to determine the values empirically [13]. This is possible with either stationary or transient methods in the laboratory. These values can, together with geotechnical parameters such as porosity or saturation, estimate the effective thermal conductivity with models as the normalized thermal conductivity models based on the work of Kersten (1949) [19] and Johansen (1975) [17]. For the thermal design of energy piles, however, it is recommended to decide these properties by field tests which is described further in chapter 2.3.1.

2.2   Soil temperature profile

The average soil temperature is often near the average air temperature. However, there are some different factors that influence these temperatures. Snow is an excellent insulator, and Ångström (1974) suggested a 1.5 °C increase in ground temperature for every 100 days with snow cover [21]. The heat island effect also refers to an increased ground temperature in more densely populated areas. In any case, the ground temperatures are generally more steady than the air temperatures as illustrated in figure 2.1.1. The upper part of the soil has seasonal fluctuations, and further down in the ground, the fluctuations tend towards a stable value.

The ground temperature measurements in figure 2.1.1 come from a test site in Halden in the southern part of Norway. A constant value from about 6-8 meters below the ground surface can be seen from Trondheim and Svalbard's similar National GeoTest Sites (NGTS). It ranges from 8 °C in Halden [22] to about 4-6 degrees in Trondheim [23] [24] and -5 °at Svalbard [25]. Similar soil temperatures is 6-11 °C for Denmark, 9-14°C for the United Kingdom and 15-19°C for Spain [12](after Geotrainet 2010).

Figure 2.2: Soil temperatures measurements in Halden (2018) from Norwegian Geo Test Sites project [22]

The stability of ground temperatures are beneficial for the GSHPS compared to air-source heat pumps (ASHP), since the ground temperature is more stable and closer to the desired temperature for buildings.
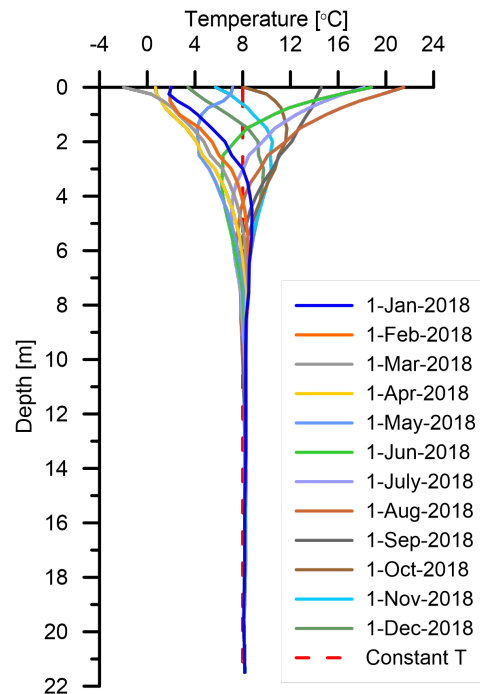
2.2.1   Freezing of the soil

Freezing of the soil can lead to the formation of ice lenses and the lifting of the soil. The freezing and thawing processes cause severe subsidence damage at buildings, foundations, and roads which leads to large economic losses [26]. Freezing is therefore not preferable concerning the normal use of energy geostructures. For this reason it is recommended that the heat carrier fluid temperature does not go below 0 °C [20].

The formation of ice lenses, which causes heave, is also especially undesirable near constructions. The formation can be large in frost susceptible soils that contain smaller grains with pore sizes with high capillarity, as silty soils. In less susceptible soils, such as very fine-grained clay, freezing can also cause fracturing of the soil and lead to increased subsidence risk [27].

Ice has higher thermal conductivity than water in the liquid phase, as shown in table 2.1. The thermal conductivity will hence ascent when the water freezes. At the same time, the latent heat of fusion can contribute with heat released by cooling. This is relevant for the use of energy geostructures in areas where freezing around the geostructure is accepted. At Svalbard, where the thawing permafrost of the active top layer is causing subsidence damage on construction, freezing of the soil is in fact beneficial. This use is investigated with numerical simulations by Helle (2021) [28].

2.3   Energy piles

The design and installation process is critical, and if done correctly, energy piles provide a viable and environment-friendly energy source [29]. See chapter 5 in appendix C for a brief introduction on energy piles.

2.3.1   Thermal design of energy piles

In the very early stage of the design process of GSHP benchmark values could be used [2]. These values are, however, very rough estimates, and as described in the sections above, there is a large variation in the thermal properties of the different soil types. There is, therefore, a need to have an in-situ field test to determine suitable values for thermal conductivity and resistances [2] [30]. It is also necessary to consider both the effect [kW] and the energy [kWh] for thermal design and to see the actual performance of GSHPs. The thermal response test (TRT), first introduced by Mogensen (1983) is a field test where the main goal is to find the *effective thermal conductivity* where also any possible convection effect is included [31]. It is executed by injecting hot water in the inlet pipe with constant power, and the temperature change over time is tracked. The pile or borehole resistance and undisturbed soil temperature can be decided by analyzing this test's data. For energy piles it is recommended with a TRT time duration of between approximately 60 and 150 hours.

There are different approaches for the thermal design of energy piles. The results of a TRT can be interpreted with several different methods. There are analytical solutions like the *infinite line source*, the *infinite cylinder*, the *infinite solid source* and their corresponding finite equivalents, and a composite model [32]. Furthermore, there are numerical models and semi-empirical models. These models were, however, originally made for deep boreholes

and do not take the internal reaction of the pile concrete, which have a larger cross-section perimeter, into account [7]. For this reason, Loverigde (2012) [7] proposed to develop concrete g-functions taking the development of pile concrete resistance into account. The different methods and the development of the thermal design of energy piles are well described in Loverigde and Powrie (2013) [8] and Alberdi-Pagola (2019) [9].

Laloui and Rotta Loria (2019) [15] recognizes the typical technological features that have some influence on the performance and can be varied in the design of energy geostructures as:

- Configuration of pipes

- Heat carrier fluid flow rate and mix

- Insulation of pipes

- Available space for connecting lines

- Position of collector and heat pumps

- Features of heat pumps

The three first items are relevant when looking just at the energy pile performance. The three last concerns are technical features above the ground and will not be discussed.

For the configuration of the pipes Laloui and Rotta Loria (2019) [15] recognized that a 2U- or a W-loop should always be preferable compared to a single U loop for maximizing the efficiency.

The heat carrier fluid is usually mixed with a antifreeze and should be adapted to the local climate. The heat carrier flow properties has though a negligible effect concerning thermomechanical behavior [15].

A particular case that is especially relevant for both colder and hotter climates is the insulation of the pipes embedded in the pile foundation. The insulation reduces the effect of the fluctuations of soil temperature and the pile wall temperature change is reduced at the upper part. This is beneficial for both the performance of the energy pile and the associated effects on the soil. [15]

Laloui and Rotta Loria (2019) [15] further described that the thermal insulation of the pipes is preventing the shallow depths where the slab is situated to be affected by the geothermal operation. And that the *slab-soil* interaction will not significantly affect the total deformation of the system, because a thermal insulation could be assumed between an upper environment and the slab floor.

2.4 Boundary condition

There are three types of boundary conditions which are often used in heat transfer [33] and computational modeling of geothermal systems [34]. The Dirichlet condition is the boundary of first kind and is identified as having a fixed surface temperature.

$$T(x_i, t) = T_i(x_i, t) \tag{2.3}$$

with x being a point on the boundary surface, and t is the time. The boundary condition of the second kind, the Neumann condition, refers to a heat flux prescribed at the surface boundary.

$$\frac{\partial T(x_i, t)}{\partial n_i} = q_{ij}(x_i, t) \tag{2.4}$$

where n_i is the normal to the boundary surface in point i, and q_{ij} is the heat flux along the surface.A special kind of this condition is when the heat flux is set to zero and is called a perfectly insulated or adiabatic condition. The third type, Cauchy, is a mix of the two mentioned conditions and reflects the condition of convection heat transfer at the boundary.

$$-\lambda \frac{\partial T}{\partial n} = h(T - T_a) \tag{2.5}$$

Where λ is the thermal conductivity, h is the heat transfer coefficient and T_a is the temperature of the ambient medium.

In numerical simulations of shallow GSHP systems, the Dirichlet surface boundary condition is often used, fixed to a constant temperature as Eskilson (1987)[35] with his g-functions described in the following section. The Cauchy type is used to simulate the effects of different atmospheric conditions at the ground surface. This is not as relevant to study for energy piles with an above-lying construction. However, the temperature fluctuations in the upper part of the soil could significantly influence the performance of the energy piles. This can be studied numerically for different conditions as Bidarmaghz et al. (2016) [36] by using Dirichlet's boundary condition and prescribing a fluctuating temperature on the ground surface and the lateral surface of the model. Alberdi-Pagola et al. (2019) [9] Loveridge and Powrie (2013) [8] used a Dirichlet constant ground temperature condition.

Olgun et al. (2015) [37] used Neumann condition with adiabatic when validating the equivalent sine wave approximation of Abdelaziz et al. (2015) [38]. Laloui and Rotta Loria (2019) [15] recommends adiabatic ground surface boundary in numerical simulation of energy piles.

2.4.1 Influence of boundary conditions

Eskilson (1987) [35] used the Dirichlet constant surface condition and discussed that the *thermal disturbance* near the ground surface was negligible. Even though this was accurate for the boreholes of an AR of 1000 and 500, the effect of ground surface temperatures is much more significant for energy piles with significantly smaller AR.

Bidarmaghz et al. (2016) [36] showed a significant effect of taking the fluctuation of surface temperature into account for energy piles, for the climate of Melbourne, Australia. The study showed 11% more efficient thermal performance for the given scenario.

Fadejev and Kurnitiski (2015) [39] showed the importance of the surface boundary condition where they used a validated 3D model and simulated a borehole field that was representing a group of energy piles in two different scenarios. The first scenario was with a borehole field placed on the side of a commercial building. This scenario

was compared to a borehole field underneath the building, which showed a 23% enhanced performance in the latter case. As Fadejev and Kurnitiski (2015) [39] states, this is also due to conduction through the floor, which causes a heat loss to the ground and a ground thermal storage effect which is beneficial for the performance of the GEPs.

2.5 G-functions

The g-functions are temperature response functions that can be used in the design of GSHP and to estimate the fluid and ground temperatures for a given heat demand and GSHP configuration. The g-functions for boreholes were introduced through the PhD work of Per Eskilson and professor Johan Claesson (1987) [35]. When looking at thermal conduction problems and the thermal response in materials, the Fourier number, Fo, is introduced. This number is a dimensionless factor of the time and for energy piles it is defined as [8] [9]:

$$Fo = \frac{\alpha_g t}{r_b^2} \tag{2.6}$$

Where α_g is the soil thermal diffusivity, t is the time since the heat flux was applied, and r_b is the equivalent radius of the pile as described in chapter 3.2.

Ground temperature response, G_g

The temperature response is also made dimensionless and is defined by [9] [8]:

$$\Phi = \frac{2\pi \lambda_g}{q} \Delta T \tag{2.7}$$

λ_g is the soil thermal conductivity, q is the heat rate injection, and ΔT is the temperature change. The temperature change, ΔT, is the difference in temperature on the pile wall, T_b, or the radial ground temperatures, $T(d_{ij})$, from the beginning of the simulation, i.e., when the heat flux was applied to the pile.

Concrete temperature response, G_c

Loverigde (2012) proposed the concrete temperature response for energy piles [7] and was introduced by Loveridge and Powrie (2013) [40]. These were applied to achieve more accurate results by implementing the transient behavior of the concrete and the fact that energy piles have different geometry and a much smaller AR than the boreholes. The concrete g-function gives the *ratio of steady-state concrete resistance* for 0.01< Fo < 10.

By taking the transient concrete into account, Loveridge and Powrie (2013) [40] showed that the performance of the pile was better, yielding less temperature change at the pile wall compared to taking the steady state concrete resistance into account. Loveridge and Powrie simulated a daily cycled heat demand, and there was a temperature difference of 2°C in the summer and 1 °C in the winter.

To finally take the transient behavior of the piles into account and derive the fluid temperatures, it is necessary to make a daily cycled heat demand as Loveridge and Powrie (2013) [8]. Loveridge and Powrie (2013) showed that, when using steady state pile resistance in the calculations, it overestimated the fluid temperatures compared to the transient behavior with concrete g-functions.

Concrete resistance, R_c

The concrete resistance, R_c is when multiplied with G_c the whole term in eq that accounts for the transient behavior of the energy pile concrete. R_c is given by:

$$R_c = \frac{T_p - T_b}{q} \tag{2.8}$$

T_p is the pipe outer wall temperature, and T_b is the pile wall temperature. The b subscript originates from borehole wall resistance and is kept in the thesis not to confuse it with the pipe wall temperature.

Pipe resistance, R_{pipe}

The pipe resistance reaches the steady state value relatively fast and is considered constant in equation 2.8 [11]. R_{pipe} is calculated with equation 2.7:

$$R_{pipe} = \frac{1}{2n\pi r_i h_i} + \frac{ln\frac{r_o}{r_i}}{2n\pi \lambda_{pipe}} \tag{2.9}$$

Where r_o is the outer and r_i is the inner pipe radius. n is the number of pipes in the cross section, and λ_{pipe} is the conductivity of the pipe. The h_i is the heat transfer coefficient, and for internal turbulent forced convection is recommended to be computed with Nusselts number using Gnielinskis correlation [11].

The pipe resistance used in the calculations is the R_{pipe} divided by the number of pipes in a cross section, n. For a single U and W shaped pile n equals 2 and 4 respectively. For the *partly* W-shape of this thesis, a ratio should be made accounting the length of the W shape at the bottom compared to the total length, deriving a n between 2 and 4.

Alberdi-Pagola et al. (2018) [11] calculated the pipe resistance values for different pipe configurations, dimensions and Reynolds number. These values can can be used when calculating fluid temperatures for energy piles.

Design temperatures

The pile wall temperature, T_b is calculated as:

$$T_b = T_0 + \frac{q}{2\pi \lambda_g} G_g \tag{2.10}$$

And the design heat carrier fluid temperature (T_f) is then computed as:

$$T_f = T_0 + \frac{q}{2\pi\lambda_g}G_g + qR_cG_c + qR_{pipe} \tag{2.11}$$

Where T_0 is the initial undisturbed ground temperature and q, λ_g, G_g, R_c, G_c, and R_{pipe} are as described above.

2.5.1 Superposition and multiple piles

As a result of the linear nature of Fourier's law and the boundary conditions being linear, the influence of adjacent piles on the performance of an energy pile can be calculated using the principle of superposition [15]. Superposition can also be applied temporal accounting for heat extraction and injection varieties. The method is described in chapter 3.5.

Loveridge and Powrie (2013) [8] introduced the multiple pile g-functions, in which Alberdi-Pagola et al. (2019) [9] adopted for the square cross-section piles.

Loveridge and Powrie (2013) found that the changes in the temperature field made by the adjacent piles did not cause any significant changes in transient or steady state pile concrete resistance. However, they found that the adjacent piles will cause adverse thermal interactions and, hence, that it is not always beneficial for the total performance to equip all piles of construction with energy piles. A highly fluctuating heat demand showed to reduce the thermal interactions between the energy piles.

The 3D FEM model of Alberdi-Pagola et al. (2018) [11] and the derived g-functions of showed good accordance with observed fluid temperatures in a case study [41] where the lowest estimated fluid temperatures reflected the measures ones.

Chapter 3

Method

3.1 Software: COMSOL Multiphysics

The software used for simulations in this thesis is the finite element method (FEM) program COMSOL Multiphysics. The FEM is a tool to compute and solve space and time-dependent problems numerically. Partial differential equations, as equation 2.1, that describe these problems mathematically are rarely possible to solve analytically for more complex geometries and boundary conditions. With numerical model equations and the FEM, there is, however, a way to approximate the solutions for different geometries and, in this way, it helps to analyze different configurations of energy piles.

The method was first used and introduced in static structural analysis with the displacement method and was afterward also applied to many different problems where problems regarding dynamic analysis, heat flux, and fluid flow were solved. A FEM-built model is divided into a geometry with a mesh of several elements where the partial differential equations are solved at the vertices (nodes). The solution derived from the FEM is approximate, but with accurate meshing and assumptions of boundary conditions and material properties, one obtains reliable results.

3.2 Model and assumptions

The model is simple and consists of three components: The quadric precast pile, the heat transfer pipes within the pile, and the surrounding soil. The soil domain is cylindrical with a diameter of 50 m, and the soil extends 25 meters below the bottom of the energy pile. The domain dimensions were chosen such that the boundary condition of the lateral surface does not affect the heat transfer of the pile and surrounding soil and are similar to the model of both Loveridge (2012) [7] and Alberdi-Pagola et al. (2019) [9].

Different meshes were tested, and a similar mesh generation as [9] was applied with user-defined mesh with the smallest elements set to 0.05 m and largest to 3.5 m. The mesh consists of tetrahedra, triangles, edge elements, and vertex elements. The pipes are modeled using the Pipe Flow Module of COMSOL [42] with water as the fluid and turbulent flow. COMSOL computes the pipe resistances, and the pile resistance is computed taking temporal

average values from the outer pipe wall and pile outer surface area.

The heat transfer in the soil and the pile concrete is simulated with pure conduction, and groundwater flow is not considered. For less permeable soils, this is a relevant assumption as discussed in chapter 2.1

Different geometries of the energy piles are studied. The aspect ratio (AR) is defined as the active thermal length of pile divided by 2*r_b:

$$AR = \frac{L_a}{2r_b}$$

The r_b is as defined in [43] the radius which provides a circumference that is equivalent to the pile perimeter.

$$r_b = \frac{2 \times \text{Pile width}}{\pi}$$

The pipes in the model have an outer diameter of 20 mm, an inner diameter of 16 mm, and hence a pipe wall thickness of 2 mm. The thermal conductivity is set as 0.42 $\frac{W}{m \times K}$. The pipes are places 6.5cm from the pipe wall, and the pile concrete extends 0.6 meters below the pipes. Parameters used to generate the ground g-functions is given in table 3.1.
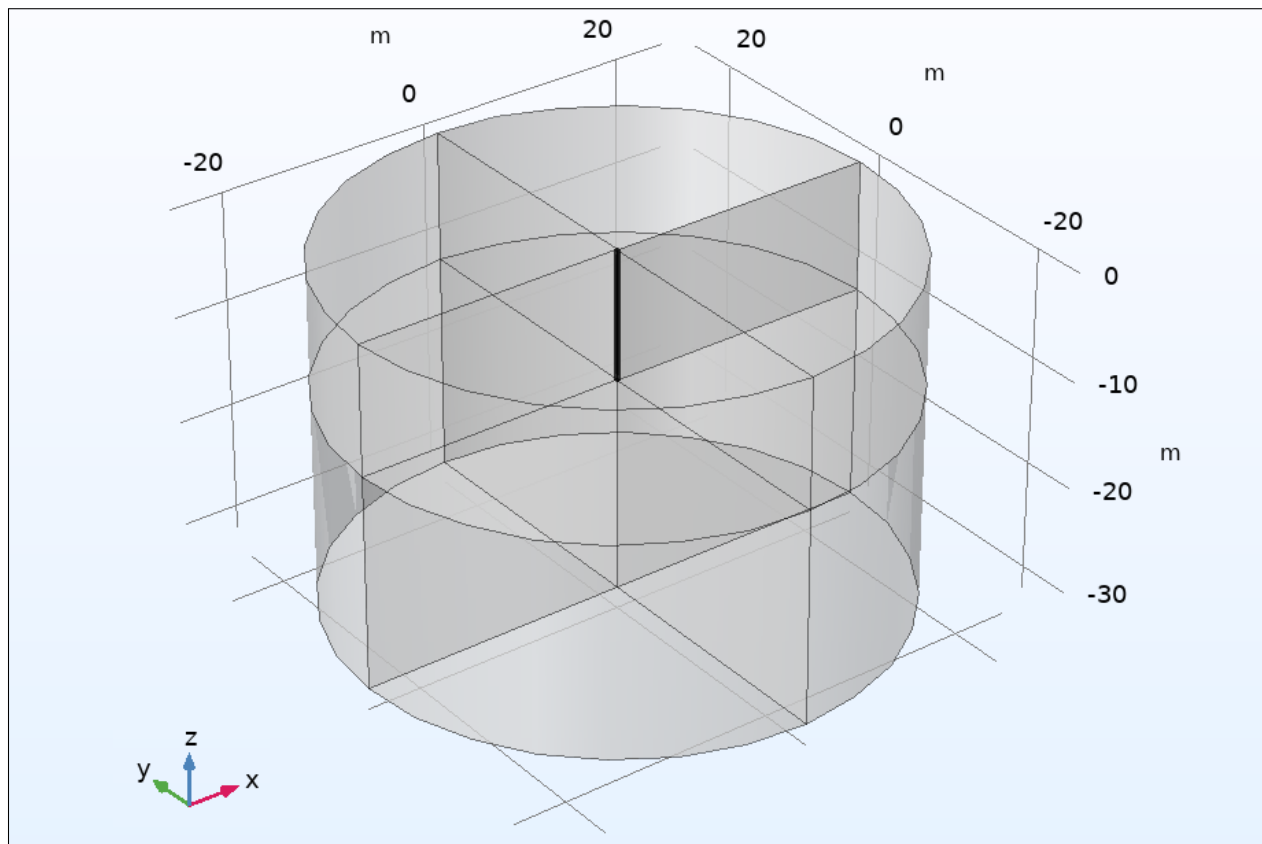

Figure 3.1: 3D FEM model with the aspect ratio of 30

Parameters	Value	
ρ_c	2000	kg/m^3
ρ_s	2000	kg/m^3
λ_c	2	$W/(mK)$
λ_s	2	$W/(mK)$
S_{cv}	2.5	$MJ/(m^3K)$
α_s	λ_s/S_{cv}	m^2/s
power	2000	W
q	power/L_a	W/m
c_p	S_{cv}/ρ	$J/(kgK)$
λ_p	0.42	$W/(mK)$
$Pipeflow$	500	l/h
$T_{undisturbed}$	8	°C

Table 3.1: Parameters for the generation of ground g-functions

The pile geometries which is studied in this thesis are the ARs of 30, 45, 60, 90, and 130. As mentioned in chapter 1 the driven square piles in Norway have a pile width of 270, 350, and 450 mm. Taken these widths and AR into account, the pile lengths can be from 15 to about 60 meters. The configuration of pipes within the piles affects the performance of the pile. Figure 3.2 shows the pipe configurations. W-shape and *partly* W-shape is the pipe configurations considered.

There was also done a done a simulation to obtain the resistances of the piles. This was done making an upper bound and lower bound for the different pile widths. The upper bound is reflected with a ratio between the conductivity of the soil , λ_s, and the conductivity of the concrete, λ_c.
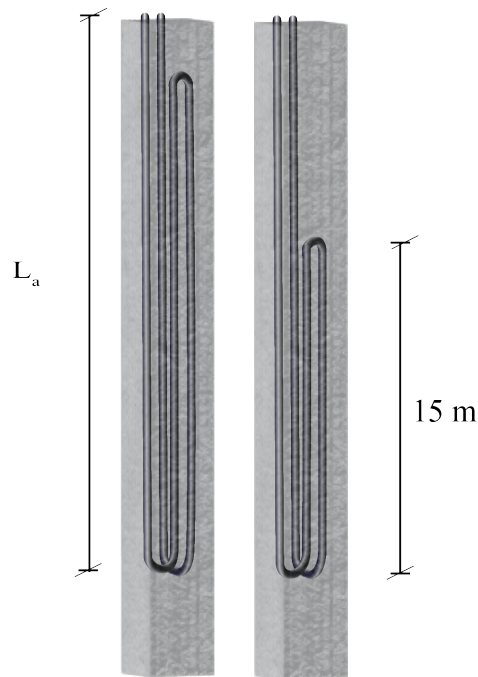
Figure 3.2: The W- and *partly* W-shaped pipe configurations.

3.2.1 Boundary conditions

There is applied an inlet flow at the defined inlet pipe which is described in chapter 3.3 and 3.4 for the different scenarios of verification and g-function generation. There is an identity boundary applied between the pile surface and surrounding soil. A constant boundary temperature is applied at the soil domain bottom and the surrounding lateral surface of the soil domain. The remaining boundary condition is the ground level surface boundary, where an adiabatic insulated boundary condition is applied. This is, together with the different AR, where the model of this thesis differs from the one of Alberdi-Pagola (2019) [9].

An intuitive assumption of the insulation boundary condition is that the building will work as an insulator as the piles will not be exposed to outdoor air or any solar radiation and that the temperature fluctuations shown in figure 2.1.1 will be affected by the building.

Assumptions:

- The soil and pile domains are homogeneous and isotropic solid materials with pure conduction heat transport.

- Domain perimeter and lateral boundary temperature is set as constant in depth and time

- Top and bottom of the whole domain is considered with adiabatic insulation

3.3 Verification of model

To verify the 3D FEM model, a TRT is simulated and verified with field test data, obtained from [43] where the TRT data and results of five quadratic driven energy piles are published. Data from the TRT of the energy pile named LM2 was used to verify the model. The test lasted for about 120 hours, where the temperature data was measured every 10 minutes. The model was calibrated with parameters from the ground thermal properties measured in the laboratory in [9].

The measured inlet temperature and the inlet pipe flow from the field test were implemented as a boundary condition at the inlet pipe of the model. Then the simulated outlet temperatures were compared with the measured outlet temperatures in the field test data as shown in figure 3.3.

The difference in the simulated and observed outlet temperatures is plotted with the corresponding values on the right y-axis. The simulation shows good accordance with the field data, especially after 10h, which would correspond to Fo $\approx$ 0.6, where the residuals are less than 0.2°C.
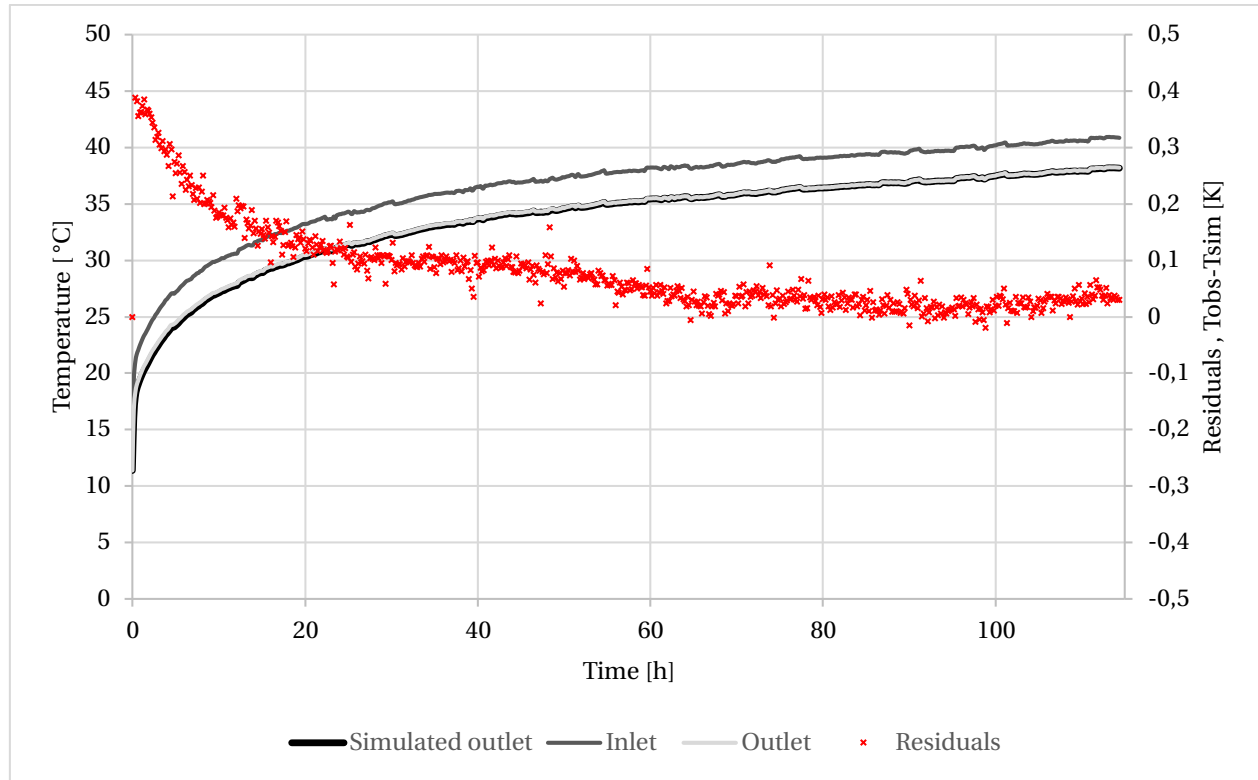
Figure 3.3: Verification of 3D FEM model with field data from Alberdi-Pagola (2018) [43].

3.4 Numerical generation of g-functions

The specific heat rate injection q [w/m] can be described as:

$$q = f S_{cv} \frac{T_{in} - T_{out}}{L_a} \tag{3.1}$$

Where f is the fluid flow rate in the pipes, S_{cv} is the volumetric heat capacity, L_a is the active length of the energy pile, T_{in} and T_{out} are respectively the inlet and outlet fluid temperatures of the pipes. By coupling the inlet to the previous step of the outlet with a constant temperature difference in the simulation, the specific heat rate injection is, as we can see from equation 3.4, also kept constant.

The heat injection is then simulated to last up to a dimensionless time, Fo = 10^4. The corresponding times of this would be between 10 and 30 years, depending on what pile width is considered.

The model of this thesis was first simulated with the constant ground surface temperature equal to the undisturbed ground temperature to validate with the model of Alberdi-Pagola (2018) [11]. It was then simulated with adiabatic ground surface temperature for the the different ARs. Then the simulated values of ϕ and Fo were curve fitted to polynomials. The radial soil temperatures was also extracted.

3.5 Superposition and multiple pile g-functions

The principle of superposition relies, as mentioned on that the heat conduction and that the specified boundary condition is linear [15]. The superposition can be applied temporally, where the variation of heat demand can be considered, and spatially, which gives the multiple pile g-functions.

The temporal variation of temperature of the fluid temperature can be calculated from the equation of Eskilson (1987) [35]. The pile wall temperature is then calculated as Spitler and Bernier (2016) [44]:

$$T_b(t_k) = T_0 + \sum_{i=1}^{k} \frac{(q_i - q_{i-1})}{2\pi\lambda_g} G_g(t_k - t_i) \tag{3.2}$$

Where k is the point in time considered. Multiple pile g-functions is not made in this thesis, but it is possible to obtain from the produced data. To obtain the multiple pile g-functions, one has to consider the radial temperatures of the ambient piles. The average temperature change at the pile wall is calculated as [8]:

$$\Delta T_b(t) = \frac{1}{n_p} \sum_{i=1}^{n_p} \sum_{j=1}^{n_p} \Delta \overline{T}(d_{ij}, t) \tag{3.3}$$

$$d_{ij} = \begin{cases} r_b & i = j \\ \sqrt{(x_i + x_j)^2 + (y_i + y_j)^2} & i \neq j \end{cases} \tag{3.4}$$

$\Delta T_b(t)$ is the mean pile wall temperature. x_i and y_i is the coordinates of pile i. n_p is the number of pile heat exchangers of the foundation. This can further be used to calculate the fluid temperatures with equation 2.11.

Chapter 4

Results

4.1 Ground g-functions

4.1.1 W-shape pipe configuration

Ground g-functions for AR30, 45, 60, 90, and 130 for W-shape. Curve fit parameters are given in appendix A. The dimensionless temperature change is increasing
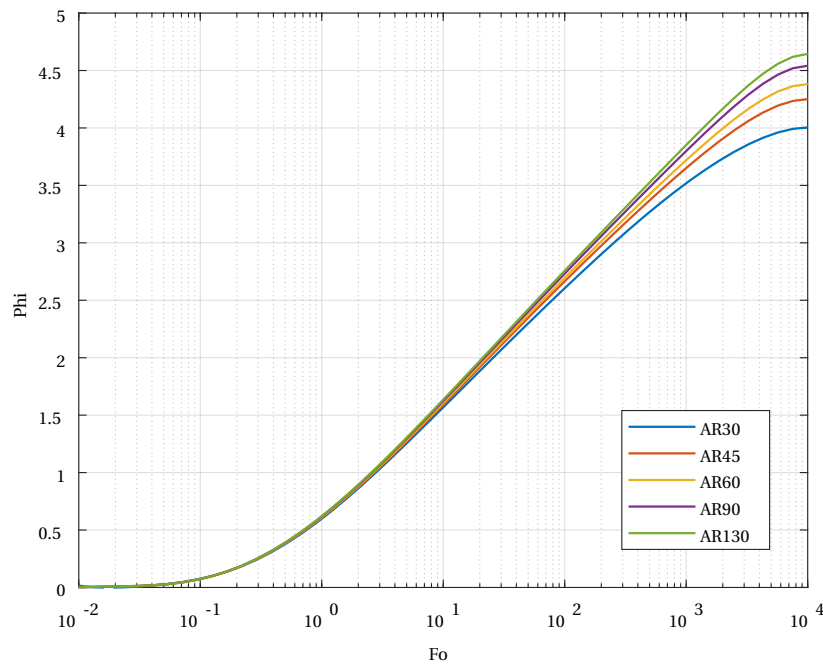
Figure 4.1: Ground g-functions for AR from 30 to 130

20

4.1.2 Partly W-shape pipe configuration

The g-functions for partly W-shaped configuration is presented in figure 4.1.2. In figure it is shown that the partly W-shape g-functions are converging at later times than W-shape. Curve fit parameters are given in appendix A.
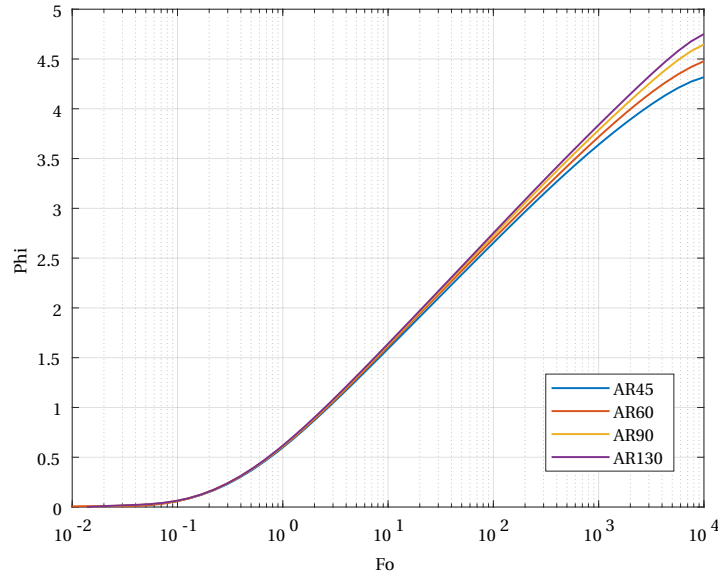
Figure 4.2: Ground g-functions for partly w-shaped pipes and AR from 30 to 130
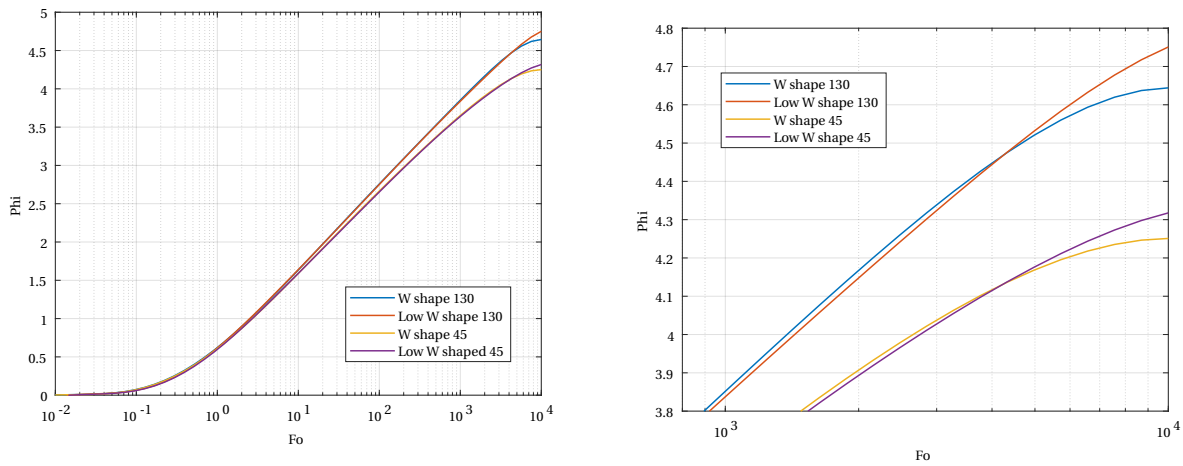
a) W-shape compared to partly w-shape of AR45 and AR130

b) Zoomed on the difference for $10^3 <$ Fo $< 10^4$

Figure 4.3: W-shape and partly w-shape g-function comparison

4.2 Radial temperature responses

Figure 4.2 is showing the temperature responses of the ground for the different AR. These ground functions can be used to obtain multiple pile functions as described in chapter 3.5.

a) AR45

b) AR60

c) AR90

d) AR130
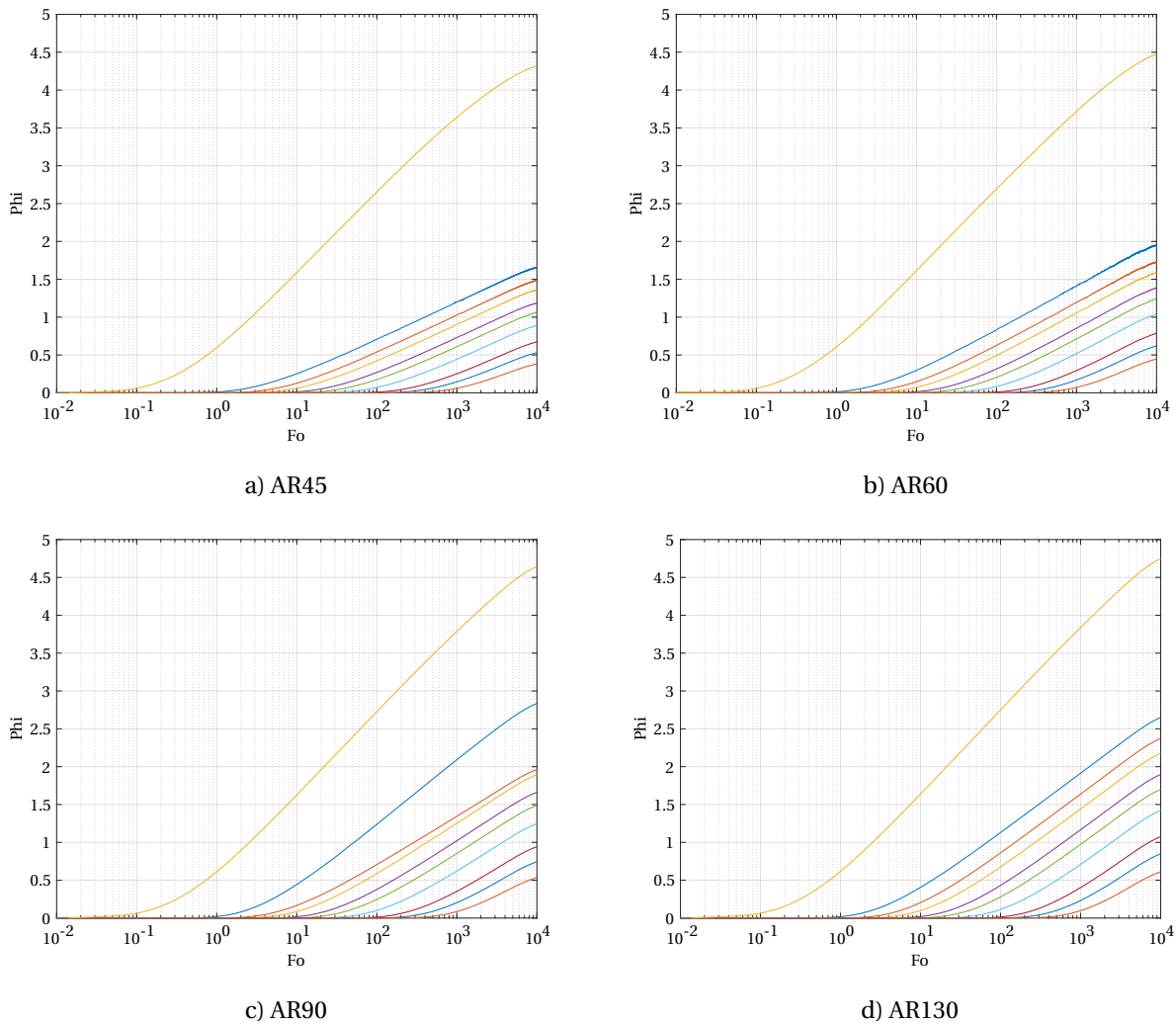
Figure 4.4: Radial temperature changes with pile wall at top and with relative distances from pile center: $S/(2*r_b)$ = 1.5, 2.2, 2.9, 4.3, 5.8, 8.7, 14.5, 20.3 and 29.

4.3   Concrete g-functions and resistance

The concrete g-functions, which is the development of the steady state pile concrete resistances, are given in figure 4.5 for 0.01 < Fo < 10. Curve fitted parameters are presented in appendix B. is given in figure 4.5. The obtained values of steady state concrete resistances are given in table 4.1. The upper bound is given by $\lambda_s/\lambda_c = 2$, and the lower bound is given by $\lambda_s/\lambda_c = 0.5$.
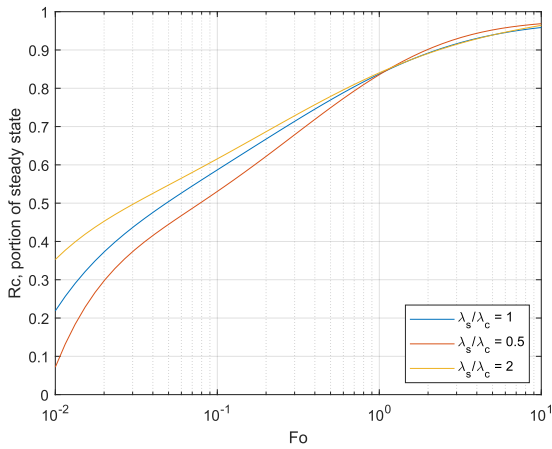
a)W-shape, 450 mm
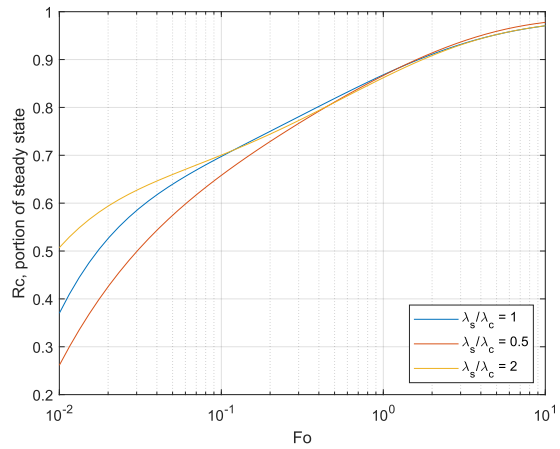
b) W-shape, 350 mm
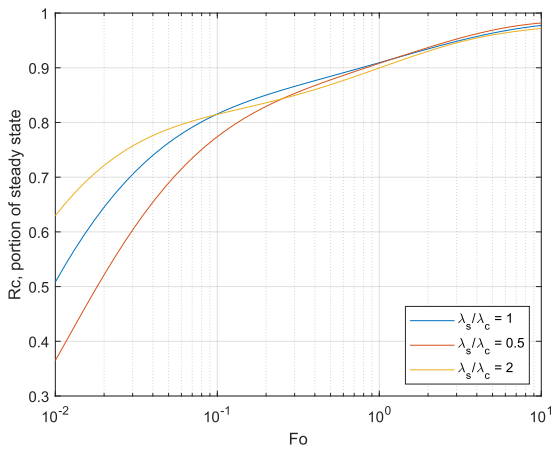
c) W-shape, 270 mm
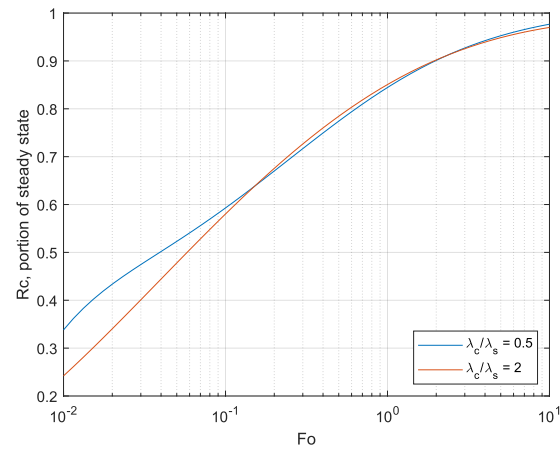
c) Partly W-shape, 270 mm

Figure 4.5: Development of steady state pile concrete resistances for the different piles and with different ratio of soil and concrete thermal conductivity

λ_s/λ_c	270 mm	350 mm	450 mm
1	0,055	0,043	0,04
0.5	0,105	0,083	0,078
2	0,059	0,045	0,041

Table 4.1: Steady state pile concrete resistance values

4.4 Pipe resistance

The pipe resistances obtained is similar to the pipe resistance diagram from Alberdi-Pagola et al. (2018) [11]. The total pipe resistance obtained for the given pipe dimensions and flow rate was 0.09 (Km)/W. For the W-shape, with $n = 4$, a pipe resistance value of 0.0225 (Km)/W can be applied. For the *partly* W-shaped configuration, the pipe resistances can be obtained by calculating the ratio where the number of pipes in the cross section, n, is a number between 2 and 4 as in the following equation:

$$n = \left(\frac{15[m]}{L_a}\right) * 2 + 2$$

4.5 Influence of boundary condition on the generation of g-functions

The model of this thesis was simulated with similar conditions as in Alberdi-Pagola et al. (2018) [11] with fixed constant ground surface temperature to validate the model and with insulated boundary condition as showed in figure 4.5 a) and b). In steady state for AR30 it was a difference of approximately 3.7%. This yields very similar calculated temperatures as shown in the scenario of figure 4.6 where the difference of temperatures is 0.13°C of the pile wall after 5 years. This difference could for example come from the meshing, a parameter, or a small difference in pile geometry.

a) AR30

b) AR45
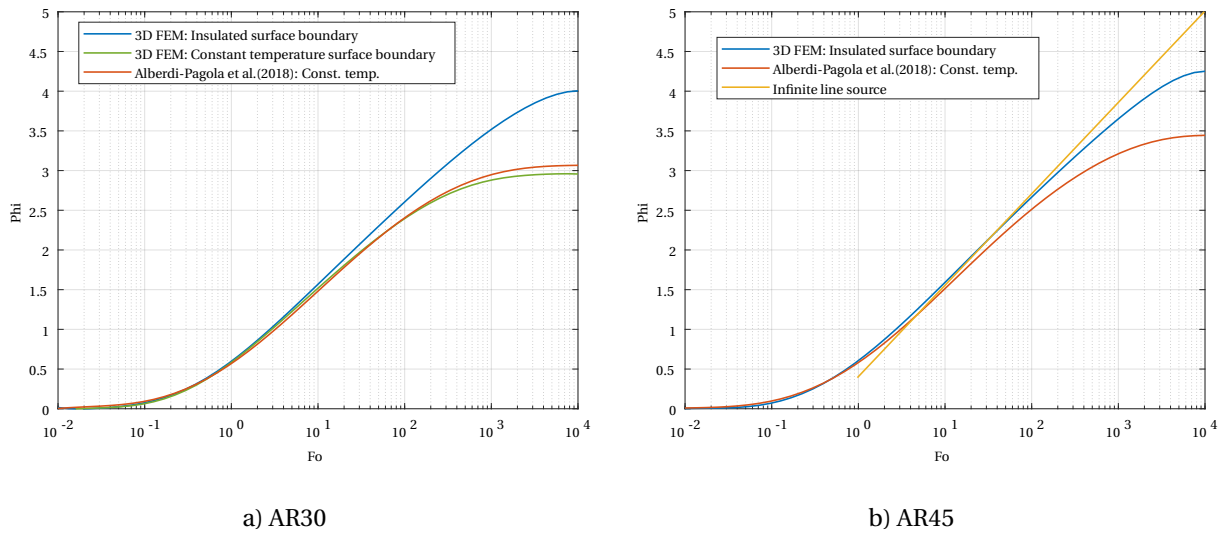
Figure 4.6: Comparison of g-functions with the different ground level surface boundary conditions: Constant temperature surface boundary condition and insulated boundary condition.

In figure 4.5 one can see that the insulated boundary model yields a higher temperature difference from about Fo = 10, which translates to about 4 to 10 days. For AR30, in figure 4.5 a), the difference is 30.6% for steady state. This difference yields more than 1°C temperature difference in the scenario shown in 4.6. For AR, in figure 4.5 b), the difference is smaller at 23.5%. The analytical solution *infinite line source* is also included in figure 4.5, showing how close the g-functions with insulated boundary condition are to this analytical solution for AR45. The g-functions of Eskilson (1987) with AR500 and AR1000 also have the same value at Fo = 10^4.

4.6 Calculation of pile wall temperatures

The method of Abdelazis et al. (2015) [38] with equivalent sine waves of thermal load is used to predict the temperature variations long-term performance on the pile wall. The equivalent sine wave is made for a single detached residential house in Norway. The calculation of these temperature changes is presented in this chapter with only the purpose of comparing the derived temperature change of the different g-functions for a fictive scenario. The Matlab code for programming the temperature changes is included in appendix B.
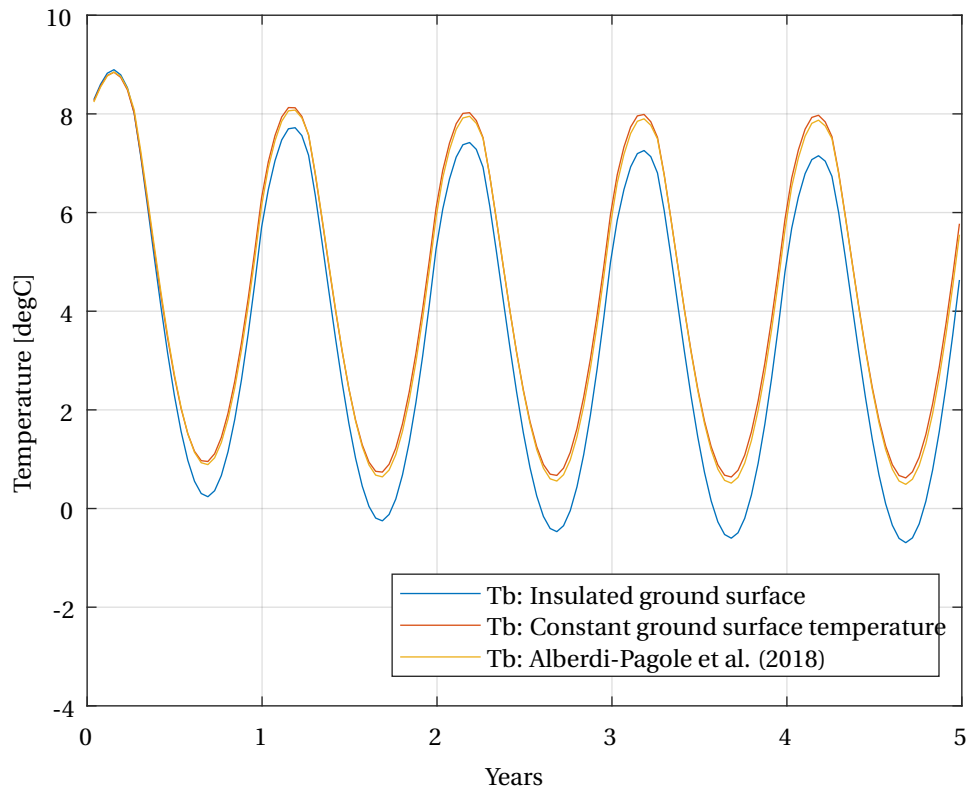
Figure 4.7: Calculated pile wall temperatures using equation 3.5
for scenario of .

Chapter 5

Discussion

As seen in figure 4.5 and 4.6, the ground level surface boundary conditions have a significant influence in the long term. The boundary conditions affect the temperature response of the ground, and hence the g-functions of the pile and the ground. In figure 5.1, the difference in the temperature distribution in the ground for the different boundary conditions, after injection of heat for about 20 years, is illustrated with isothermal contours.

(a) Adiabatic insulation   (b) Constant temperature
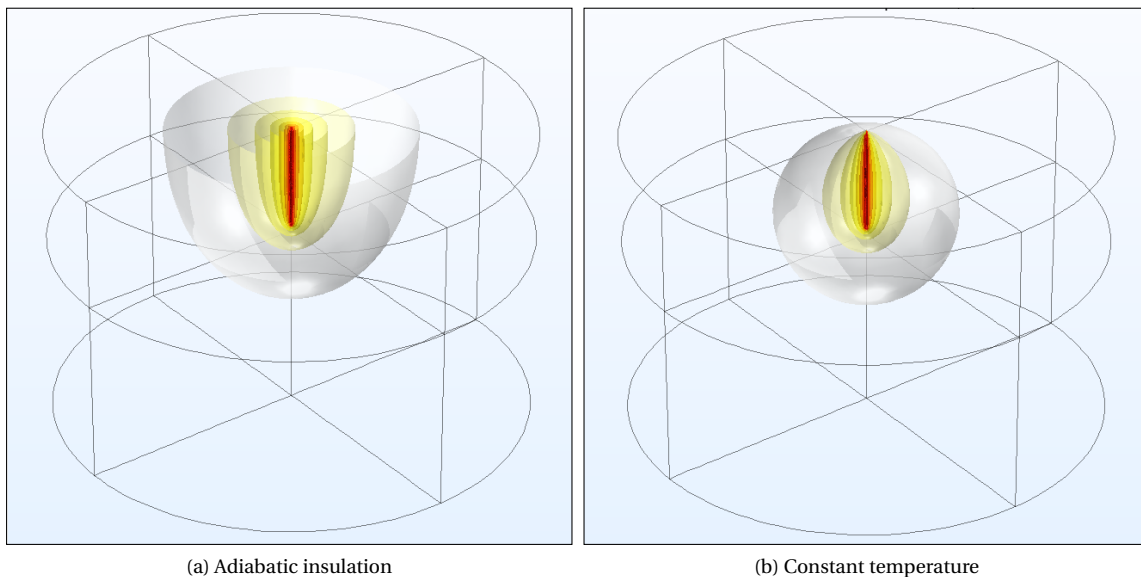
Figure 5.1: Isothermal contours after heat injection with different boundary conditions

Regarding energy piles with a shorter AR than boreholes, we will see in chapter 4 that the boundary conditions seem to influence the performance a lot. When regarding larger ARs, this has presumably lessened effect, considering that the AR45 has less difference than AR30.

It was shown from the verification of the model in chapter 3.3 that the model is accurate in estimating the ground thermal responses for short times. The 3D FEM model with insulated boundary is compared to the 3D FEM model with constant temperature, and other analytical solutions in figure 5, with graphs obtained from Alberdi-

Pagola et al. (2017) [32]. This shows that the insulated boundary condition places the model of this thesis in between the infinite sources and the finite solid cylinder source in the long term.

The g-functions with insulated boundary surface condition yields higher temperature change than constant temperature surface boundary, and the g-functions could therefore be overestimating the long term critical change in fluid temperature during the winter in a colder climate and underestimating the thermal performance of the pile. A proposal for a method yielding lower temperature change for calculating the long-term performance with the g-functions presented in this thesis could be combining the g-functions for Fo < 10 and then apply the corresponding analytical solution of the finite solid cylinder source, of the pile, for long-term analysis.

Laloui and Rotta Loria (2019) recommended using adiabatic conditions for the ground surface boundary conditions. These recommendations are mentioned in relation to the fact that the influence of the daily fluctuating temperature in the upper part of the soil is negligible in the context of the total deformation of the piles.

The assumption of insulated boundary conditions in a long-term analysis could yield a conservative estimate for the thermal performance of a pile, considering the simulated g-functions in this thesis.
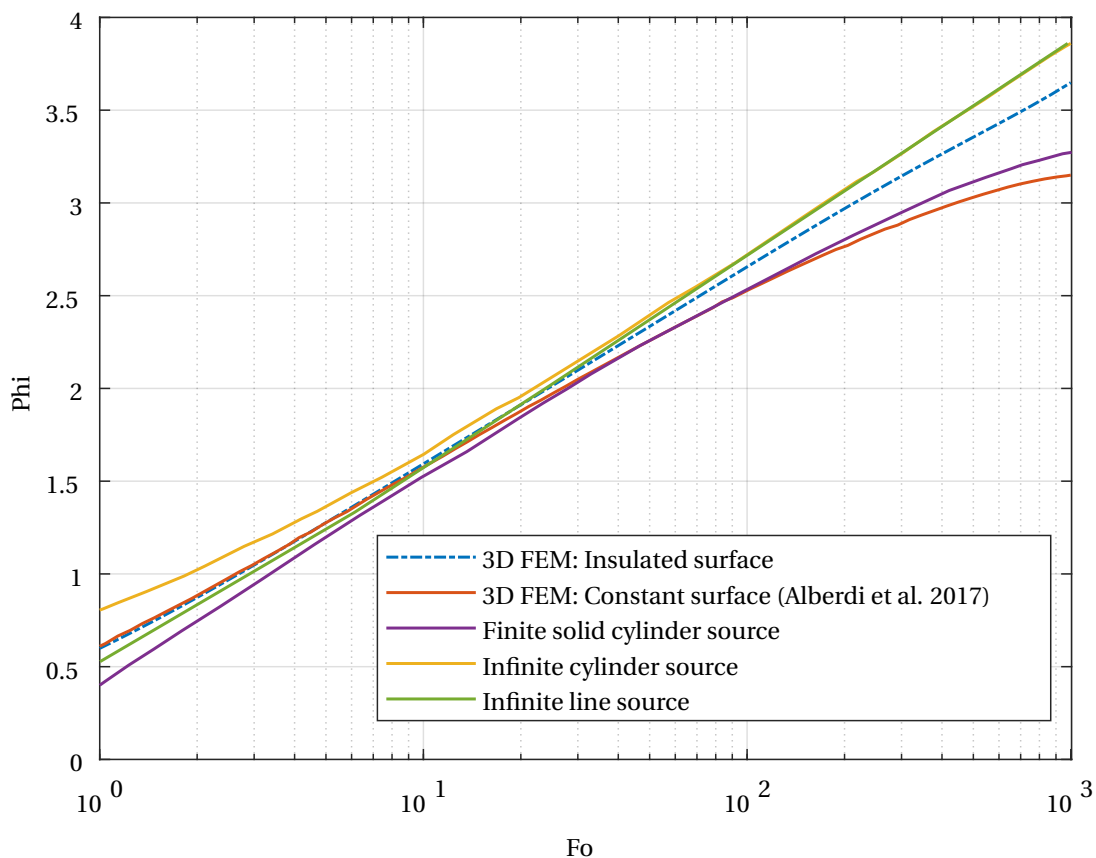
Figure 5.2: Long term comparison of the pile g-functions. [32]

The thermal design is critical in a cold, nordic climate with excess thermal heat extraction and subsidence risk if the soil freezes. Laloui and Rotta Loria (2019) state that insulating the pipes is good practice. This could enhance the performance of the piles in the cold climate of Norway, where the upper part of the soil can be affected by the cold air temperatures. Some factors can contribute to the performance of energy piles, depending on the climatic and ground conditions. The effects of heat conduction through the floor of a building [39], intermittent thermal load, fluctuations of upper soil [36] and groundwater flow can contribute to the performance of the piles.

To obtain accurate fluid temperature values for shorter terms and to account for the thermal storage in the piles and the transient behavior of the piles, a daily cycled heat load should be implemented in the calculations, as Loveridge and Powrie (2013) [40]. This was shown to be beneficial for the design and thermal performance of the energy piles.

Chapter 6

Conclusion

In the work of this thesis, semi-empirical g-functions for precast concrete energy piles with the AR of 30 to 130 were simulated using a 3D FEM model. The AR is longer than earlier investigated, considering energy pile segments of 15 meters that can be joined. The model was based on the assumptions of a pure conduction heat transfer in the concrete and soil, and specifically an adiabatic insulated ground level surface boundary condition. These simulations were compared to the g-functions obtained by Alberdi-Pagola et al. (2018) [11], which had a ground level surface boundary condition set to a constant temperature.

The different pipe configurations investigated were W-shape and *partly* W-shaped. The ground g-functions for these two configurations were similar, but *partly* W-shape was yielding higher values for Fourier number, Fo $> 5 * 10^3$. The concrete functions for the different ground conditions and pipe configurations are presented. The concrete g-functions serve as a method to calculate more accurate fluid temperatures and can be used to obtain daily fluctuating fluid temperatures within the pile.

Compared to the g-functions of Alberdi-Pagola et al. (2018) [11], the g-functions of this thesis were yielding similar values of the dimensionless temperature, ϕ, for Fo < 10, which is within a typical time scope of a TRT test for energy piles. For higher values of Fo, the insulated g-functions yielded higher values of ϕ. At Fo = 10^4, the difference for energy piles with AR30 was 30.6%, and for AR45, it was 23.5%. This difference leads to higher estimated temperature differences from the insulated g-functions when calculating pipe wall temperatures or fluid temperatures.

However, to obtain long-term g-functions, the model has to be simple. There are many factors influencing the performance of an energy pile that the 3D FEM model of this thesis does not consider. These factors can be forced convection from the groundwater flow present in the soil, conduction through the above-lying slab, and soil temperature fluctuations. Many of these factors are beneficial for the performance of a GSHP system and the regeneration of the soil.

The temperatures in the upper part of the soil can affect the performance of an energy pile, especially in the winter, where it is critical that the ground surrounding the piles does not freeze. Because of this, it is recommended to have a minimum fluid temperature of 0 °C. Considering the transient behavior of the pile and the heat stored

within the pile concrete, the fluid temperature could go below 0°C without the soil freezing. This could be investigated in the context of the design of the energy piles. Another recommendation for further work is the insulation of the pipes for the upper 4-5 meters of the pile. Is the insulation possible to apply for the driven concrete piles of smaller cross sections in regards to the capacity, and how does it influence the performance of the pile?

As the g-functions of this thesis yield significantly higher temperature changes for the calculated pile wall temperatures, they can be considered an extreme case and possibly yields conservative design values. However, the assumption of an insulated surface gives good results in the short term. The model is verified with a TRT test, and the g-functions could therefore also serve as a reasonable interpretation method for TRTs of energy piles, such as for Alberdi-Pagola et al. (2018, 2019) in the work of validating the g-functions as a preferable design method. [43] [32] [9].

Bibliography

[1] H. Brandl, "Geothermal Geotechnics for Urban Undergrounds," *Procedia Engineering*, vol. 165, pp. 747–764, 1 2016.

[2] L. Helsen, "Geothermally activated building structures," in *Advances in Ground-Source Heat Pump Systems* (S. Rees, ed.), ch. 15, pp. 423–453, 2016.

[3] R. K. Ramstad, "Grunnvarme i Norge - kartlegging av økonomisk potensial," tech. rep., Norwegian Water Resources and Energy Directorate (NVE), 2011.

[4] J. W. Lund and A. N. Toth, "Direct Utilization of Geothermal Energy 2020 Worldwide Review," tech. rep.

[5] "Asplan Viak/ Oslo economics, Kartlegging og vurdering av potensial for effektivisering av oppvarming og kjøling i Norge," tech. rep., Norwegian Water Resources and Energy Directorate (NVE), 2019.

[6] O. S. Lillevold, "Potential of geothermal energy piles in Norway," in *[Unpublished specialization project]*, 2021.

[7] F. Loveridge, "The thermal performance of foundation piles used as heat exchangers in ground energy systems," 2012.

[8] F. Loveridge and W. Powrie, "G-Functions for multiple interacting pile heat exchangers," 2013.

[9] M. Alberdi-Pagola, S. E. Poulsen, R. L. Jensen, and S. Madsen, "Thermal design method for multiple precast energy piles," *Geothermics*, vol. 78, pp. 201–210, 3 2019.

[10] Den norske Pelekomité, *PELEVEILEDINGEN*. Norwegian Geotechnical Society, 2019.

[11] M. Alberdi, R. Lund, and S. Erbs, "Method to obtain g-functions for multiple precast quadratic pile heat exchangers," tech. rep., Aalborg Universitet , Department of Civil Engineering, 2018.

[12] D. Banks, *An Introduction to Thermogeology: Ground Source Heating and Cooling*. 2 ed., 2012.

[13] Johansen, "VARMETEKNISKE EGENSKAPER AV JORD OG BYGNINGSMATERIALER," in *Frost action in soils*, ch. 4, pp. 73–118, Oslo: Committee on Frost Action in Soils, 17 ed., 1976.

[14] S. W. Rees, M. H. Adjali, Z. Zhou, M. Davies, and H. R. Thomas, "Ground heat transfer effects on the thermal performance of earth-contact structures," *Renewable and Sustainable Energy Reviews*, vol. 4, pp. 213–265, 9 2000.

[15] L. Laloui and A. F. Rotta Loria, *Analysis and Design of Energy Geostructures: Theoretical essentials and practical application.* 1 ed., 2019.

[16] O. T. Farouki, "Thermal properties of soils ," tech. rep., 1981.

[17] Johansen, *Thermal Conductivity of Soils.* PhD thesis, NTH, 7 1975.

[18] A. Chiasson, S. Rees, and J. Spitler, "A preliminary assessment of the effects of groundwater flow on closed-loop ground source heat pump systems," 2000.

[19] M. S. Kersten, "Thermal Properties of Soils," 6 1949.

[20] "Thermal use of the underground," in *VEREIN DEUTSCHER INGENIEURE RICHTLINIEN- VDI 4640 (English issue)*, 2010.

[21] B. Rosén, A. Gabrielsson, J. Fallsvik, G. Hellström, and G. Nilsson, *System för värme och kyla ur mark - En nulägesbeskrivning.* Linköping: Swedish Geothechnical Institute, 2001.

[22] Øyvind Blaker, "Norwegian GeoTest Sites (NGTS): Halden research site - Site characterisation and engineering properties of Halden silt," tech. rep., NGI, 10 2019.

[23] J.-S. L Heureux, A. Lindgård, and A. Emdal, "The Tiller-Flotten research site: Geotechnical characterization of a very sensitive clay deposit," *831-867*, vol. 5, no. 4, pp. 831–867, 2019.

[24] S. Quinteros, A. Gundersen, J. S. L'Heureux, and R. Carraro, J. Antonio H. Jardine, "Norwegian GeoTest Sites (NGTS): Øysand researche site - geotechnical characterization of deltaic sandy-silty soils," tech. rep., Research Council of Norway (RCN), 2019.

[25] G. L. Gilbert, A. Instanes, A. Sinitsyn, and A. Aalberg, "Norwegian GeoTest Sites (NGTS): Characterisation of two sites for getechnical testing in permafrost Longyearbyen, Svalbard," tech. rep., Research Council of Norway (RCN), Longyearbyen, 2019.

[26] R. Sætersdal, "PROBLEMER VED FRYSING AV JORD. FORSKNINGSAKTIVITET," in *Frost action in soils*, ch. 1, pp. 11–18, Oslo: Committee on Frost Action in Soils, 17 ed., 1976.

[27] B. Brattli, *PENSUMHEFTE: Ingeniørgeologi, løsmasser.* Akademika, 2019.

[28] S. T. Heller, "A Numerical Simulation of Permafrost Thermal Regime under a Heat Pump Chilled Foundation in Longyearbyen, Svalbard," 2021.

[29] A. K. Sani, R. M. Singh, T. Amis, and I. Cavarretta, "A review on the performance of geothermal energy pile foundation, its design process and applications," *Renewable and Sustainable Energy Reviews*, vol. 106, no. July 2018, pp. 54–78, 2019.

[30] H. Witte, "In situ estimation of ground thermal properties," in *Advances in Ground-Source Heat Pump Systems* (S. Rees, ed.), ch. 4, 2016.

[31] S. Gehlin, "Thermal response test : method development and evaluation," 2002.

[32] M. Alberdi-Pagola, S. E. Poulsen, F. Loveridge, S. Madsen, and R. L. Jensen, "Comparing heat flow models for interpretation of precast quadratic pile heat exchanger thermal response tests," *Energy*, vol. 145, pp. 721–733, 2 2018.

[33] T. L. Bergman, A. S. Lavine, F. P. Incropera, and D. P. DeWitt, *Fundamentals of Heat and Mass Transfer, Seventh Edition Binder Ready Version.* 2011.

[34] R. Al-Khoury, "Computational modeling of shallow geothermal systems," p. 233, 2012.

[35] P. Eskilson, *Thermal Analysis of Heat Extraction Boreholes.* PhD thesis, 1987.

[36] A. Bidarmaghz, G. A. Narsilio, I. W. Johnston, and S. Colls, "The importance of surface air temperature fluctuations on long-term performance of vertical ground heat exchangers," *Geomechanics for Energy and the Environment*, vol. 6, pp. 35–44, 6 2016.

[37] C. G. Olgun, T. Y. Ozudogru, S. L. Abdelaziz, and A. Senol, "Long-term performance of heat exchanger piles," *Acta Geotechnica*, vol. 10, pp. 553–569, 10 2015.

[38] S. L. Abdelaziz, C. G. Olgun, and J. R. Martin, "Equivalent energy wave for long-term analysis of ground coupled heat exchangers," *Geothermics*, vol. 53, pp. 67–84, 1 2015.

[39] J. Fadejev and J. Kurnitski, "Geothermal energy piles and boreholes design with heat pump in a whole building simulation software," *Energy and Buildings*, vol. 106, pp. 23–34, 11 2015.

[40] F. Loveridge and W. Powrie, "Temperature response functions (G-functions) for single pile heat exchangers," *Energy*, vol. 57, pp. 554–564, 8 2013.

[41] M. Alberdi-Pagola, S. E. Poulsen, R. L. Jensen, and S. Madsen, "A case study of the sizing and optimisation of an energy pile foundation (Rosborg, Denmark)," *Renewable Energy*, vol. 147, pp. 2724–2735, 3 2018.

[42] COMSOL, "Pipe Flow Module User's Guide," www.comsol.com, 2018.

[43] M. Alberdi-Pagola, "Thermal response test data of five quadratic cross section precast pile heat exchangers," *Data in Brief*, vol. 18, pp. 13–15, 6 2018.

[44] J. D. Spitler and M. Bernier, "Vertical borehole ground heat exchanger design methods," *Advances in Ground-Source Heat Pump Systems*, pp. 29–61, 1 2016.

Appendix A

Curve fitting parameters

A.1 Ground g-functions: W-shape

This is the curve fitting parameters to the obtained from curve fitting of the simulated data. Valid from 0.01 < Fo < 10 000.

$$
\begin{aligned}
G_g(Fo) = {} & a * log(Fo)^9 + b * log(Fo)^8 + c * log(Fo)^7 + d * log(Fo)^6 + e * log(Fo)^5 \\
& + f * log(Fo)^4 + g * log(Fo)^3 + h * log(Fo)^2 + i * log(Fo) + j
\end{aligned}
\tag{A.1}
$$

	AR30	AR45	AR60	AR90	AR130
a	-0,0000411	-0,00001413	-0,00001961	-0,00002705	-0,00003002
b	0,0004693	0,0001455	0,0001797	0,0002338	0,0002456
c	-0,001516	-0,0004731	-0,0004756	-0,0005391	-0,0004948
d	-0,001678	-0,001004	-0,001326	-0,001655	-0,00184
e	0,01727	0,01006	0,01054	0,01144	0,01132
f	-0,01682	-0,01255	-0,01166	-0,01144	-0,01061
g	-0,084	-0,07059	-0,07221	-0,07418	-0,07411
h	0,2422	0,2389	0,2411	0,2447	0,2459
i	0,8146	0,8209	0,8285	0,8378	0,8435
j	0,5977	0,6063	0,6106	0,617	0,6207
RMSE	0,01786	0,003988	0,001757	0,001883	0,001939
R^2	0,9995	1	1	1	1
SSE	1,277	0,06368	0,01236	0,01419	0,01504

Table A.1

A.2 Ground g-functions: Partly W-shaped

The polynomial, such as A.1, applies for the partly W-shaped g-functions, and it is also valid for 0.01 < Fo < 10 000.

	AR45	**AR60**	**AR90**	**AR130**
a	-0,00005629	-0,00001279	-0,00006402	-0,00006935
b	0,0005636	0,0001738	0,0006048	0,000644
c	-0,001253	-0,0006501	-0,00119	-0,001208
d	-0,004378	-0,001388	-0,004934	-0,005334
e	0,02038	0,01294	0,02078	0,02138
f	-0,005522	-0,01135	-0,003642	-0,002315
g	-0,1039	-0,0852	-0,1062	-0,1082
h	0,2374	0,2424	0,2414	0,2418
i	0,8494	0,8502	0,8689	0,876
j	0,5972	0,6061	0,6117	0,6169
RMSE	*0,01271*	*0,02034*	*0,000978*	*0,0006425*
R^2	*0,9998*	*0,9996*	*1*	*1*
SSE	*0,3953*	*1,012*	*0,00234*	*0,00101*

Table A.2

A.3 Concrete g-functions

```
1   %% Concrete resistances, for different soil and concrete conductivity ratios
2   %% 450 mm pile — ks 2, kc 2
3   %Linear model Poly6:
4   %    Coefficients (with 95% confidence bounds):
5         p1 =    0.002486;%   (0.002104, 0.002867)
6         p2 =    0.005627;%   (0.005034, 0.006221)
7         p3 =   −0.01836;%   (−0.02016, −0.01657)
8         p4 =   −0.008668;%  (−0.01077, −0.006564)
9         p5 =    0.003045;   %(0.0008639, 0.005226)
10        p6 =     0.08395;   %0.08228, 0.08563)
11        p7 =      0.9093;%   (0.9088, 0.9098)
12        x = logspace(−2,1);
13      rc = p1.*log10(x).^6 + p2.*log10(x).^5 + p3.*log10(x).^4 + p4.*log10(x).^3 + p5.*log10(x).^2 + p6.*log10(x) + p7;
14  %% 350 mm pile — ks 2, kc 2
15        p12 =    −0.00135 ;% (−0.001806, −0.0008945)
16        p22 =    0.006847 ;% (0.006389, 0.007306)
17        p32 =     0.00343;%  (0.001048, 0.005811)
18        p42 =    −0.02606 ;% (−0.02804, −0.02409)
19        p52 =    −0.03612 ;% (−0.0391, −0.03314)
20        p62 =     0.1557;%   (0.154, 0.1574)
21        p72 =     0.8681;%   (0.8675, 0.8686)
22      rc2 = p12.*log10(x).^6 + p22.*log10(x).^5 + p32.*log10(x).^4 + p42.*log10(x).^3 + p52.*log10(x).^2 + p62.*log10(x) + p72;
23  %% 270 mm pile — ks 2, kc 2
24        p13 =   −0.002265;%  (−0.00276, −0.00177)
25        p23 =    0.005575 ;% (0.004696, 0.006455)
26        p33 =     0.0137;%   (0.01144, 0.01596)
27        p43 =   −0.02514;%   (−0.02821, −0.02207)
28        p53 =   −0.07616;%   (−0.07912, −0.0732)
29        p63 =     0.2055 ;%  (0.2035, 0.2075)
30        p73 =     0.8375;%   (0.8368, 0.8382)
31      rc3 = p13.*log10(x).^6 + p23.*log10(x).^5 + p33.*log10(x).^4 + p43.*log10(x).^3 + p53.*log10(x).^2 + p63.*log10(x) + p73;
32      %% 450 mm pile — ks 2, kc 1
33        p14 =    0.005072;%  (0.00463, 0.005514)
34        p24 =    0.004948;%  (0.00426, 0.005636)
35        p34 =   −0.03039;%   (−0.03247, −0.02831)
36        p44 =    0.001016;%  (−0.001421, 0.003454)
37        p54 =   −0.004827;%  (−0.007355, −0.0023)
38        p64 =     0.09794;%  (0.09599, 0.09988)
39        p74 =     0.9081;%   (0.9076, 0.9087)
40      rc4 = p14.*log10(x).^6 + p24.*log10(x).^5 + p34.*log10(x).^4 + p44.*log10(x).^3 + p54.*log10(x).^2 + p64.*log10(x) + p74;
41      %% 350 mm pile — ks 2, kc 1
42        p15 =   0.0004498;%  (−9.691e−05, 0.0009964)
43        p25 =    0.005488;%  (0.004938, 0.006039)
44        p35 =   −0.005011;%  (−0.007867, −0.002155)
45        p45 =    −0.01782;%  (−0.02019, −0.01546)
46        p55 =    −0.04414;%  (−0.04771, −0.04056)
47        p65 =     0.1721;%   (0.17, 0.1741)
48        p75 =     0.8666;%   (0.866, 0.8673)
49        rc5 = p15.*log10(x).^6 + p25.*log10(x).^5 + p35.*log10(x).^4 + p45.*log10(x).^3 + p55.*log10(x).^2 + p65.*log10(x) + p75
50      %% 270 mm pile — ks 2, kc 1
51        p16 =   −0.006206;%  (−0.006816, −0.005597)
52        p26 =     0.01065;%  (0.00957, 0.01174)
```

```
53        p36 =      0.03447;%  (0.03169, 0.03726)
54        p46 =     −0.04932;%  (−0.0531, −0.04554)
55        p56 =      −0.1141;%  (−0.1177, −0.1104)
56        p66 =       0.2577;%  (0.2552, 0.2601)
57        p76 =       0.8355;%  (0.8347, 0.8363)
58        rc6 = p16.*log10(x).^6 + p26.*log10(x).^5 + p36.*log10(x).^4 + p46.*log10(x).^3 + p56.*log10(x).^2 + p66.*log10(x) + p76
59        %% 450 mm pile — ks 1, kc 2
60        p17 =     0.003698;%  (0.003272, 0.004123)
61        p27 =      0.01393 ;% (0.01259, 0.01528)
62        p37 =     −0.01124;%  (−0.01246, −0.01003)
63        p47 =     −0.04051;%  (−0.04393, −0.03708)
64        p57 =     0.001329;%  (−0.0007957, 0.003454)
65        p67 =       0.1052;%  (0.1032, 0.1073)
66        p77 =       0.8996;%  (0.8988, 0.9005)
67        rc7 = p17.*log10(x).^6 + p27.*log10(x).^5 + p37.*log10(x).^4 + p47.*log10(x).^3 + p57.*log10(x).^2 + p67.*log10(x) + p77
68        %% 350 mm pile — ks 1, kc 2
69        p18 =    0.0002701;%  (−0.000205, 0.0007452)
70        p28 =     0.009062 ;% (0.00813, 0.009994)
71        p38 =     0.003034;%  (0.001023, 0.005046)
72        p48 =     −0.04011 ;% (−0.04314, −0.03707)
73        p58 =     −0.02978 ;% (−0.03224, −0.02733)
74        p68 =       0.1662;%  (0.164, 0.1684)
75        p78 =        0.862 ;% (0.8613, 0.8626)
76        rc8 = p18.*log10(x).^6 + p28.*log10(x).^5 + p38.*log10(x).^4 + p48.*log10(x).^3 + p58.*log10(x).^2 + p68.*log10(x) + p78
77        %% 270 mm pile — ks 1, kc 2
78        p19 =    −0.002576 ;% (−0.003008, −0.002144)
79        p29 =     0.002108 ;% (0.001653, 0.002563)
80        p39 =      0.01567;%  (0.01344, 0.0179)
81        p49 =      −0.0154 ;% (−0.0173, −0.01351)
82        p59 =     −0.06349 ; %(−0.06626, −0.06072)
83        p69 =       0.1876;%  (0.1859, 0.1893)
84        p79 =       0.8404 ;% (0.8399, 0.8409)
85        rc9 = p19.*log10(x).^6 + p29.*log10(x).^5 + p39.*log10(x).^4 + p49.*log10(x).^3 + p59.*log10(x).^2 + p69.*log10(x) + p79
86        %% Low W shaped bottom upper limit (270 mm) —  ks 1, kc 2
87        p110 =    −0.003438;%  (−0.005706, −0.001169)
88        p210 =    0.002349 ;% (−0.002062, 0.00676)
89        p310 =     0.02104;%  (0.01419, 0.02788)
90        p410 =    −0.02342 ;% (−0.03354, −0.01331)
91        p510 =     −0.0773  ;%(−0.08383, −0.07076)
92        p610 =       0.213;%  (0.2081, 0.2179)
93        p710 =      0.8445 ;% (0.8435, 0.8455)
94 rc10 = p110.*log10(x).^6 + p210.*log10(x).^5 + p310.*log10(x).^4 + p410.*log10(x).^3 + p510.*log10(x).^2 + p610.*log10(x) + p710
95        %% Low W shaped lower
96        p111 =   −0.0002204;%  (−0.0002889, −0.0001519)
97        p211 =   −0.0003383;%  (−0.000519, −0.0001577)
98        p311 =    0.007061;%  (0.006183, 0.00794)
99        p411 =   −0.0002831;%  (−0.001828, 0.001261)
100       p511 =      −0.0824;%  (−0.08562, −0.07917)
101       p611 =       0.1955;%  (0.1924, 0.1987)
102       p711 =       0.8507;%  (0.8493, 0.8521)
103       rc11 = p111.*log10(x).^6 + p211.*log10(x).^5 + p311.*log10(x).^4 + p411.*log10(x).^3 + p511.*log10(x).^2 + p611.*log10(x) +
              p711
104
105    semilogx(x,rc4,x,rc7,x,rc)
```

```matlab
106        grid on
107        xlabel('Fo')
108        ylabel('Rc, portion of steady state')
109        legend('\lambda_c/\lambda_s = 0.5','\lambda_c/\lambda_s = 2 ','\lambda_c/\lambda_s = 1','Location','southeast')
110  %      nexttile
111        semilogx(x,rc5,x,rc8,x,rc2)
112        grid on
113        xlabel('Fo')
114        ylabel('Rc, portion of steady state')
115        legend('\lambda_c/\lambda_s = 0.5','\lambda_c/\lambda_s = 2 ','\lambda_c/\lambda_s = 1','Location','southeast')
116  %  nexttile
117        semilogx(x,rc6,x,rc9,x,rc3)
118        grid on
119        xlabel('Fo')
120        ylabel('Rc, portion of steady state')
121        legend('\lambda_c/\lambda_s = 0.5','\lambda_c/\lambda_s = 2 ','\lambda_c/\lambda_s = 1','Location','southeast')
122  %      nexttile
123        semilogx(x,rc6,x,rc9,x,rc3)
124        grid on
125        xlabel('Fo')
126        ylabel('Rc, portion of steady state')
127        legend('\lambda_c/\lambda_s = 0.5','\lambda_c/\lambda_s = 2 ','\lambda_c/\lambda_s = 1','Location','southeast')
128   % nexttile
129         semilogx(x,rc10,x,rc11)
130        grid on
131        xlabel('Fo')
132        ylabel('Rc, portion of steady state')
133        legend('\lambda_c/\lambda_s = 0.5','\lambda_c/\lambda_s = 2 ','Location','southeast')
```

Appendix B

Calculation of pile wall temperatures

```matlab
1  %% Calculation of energy pile wall temperature for  time-varying heat demand
2          p1 =    -4.11e-05; % (-7.01e-05, -1.21e-05)   %Curve fitting parameters
3          p2 =   0.0004693; % (0.0001285, 0.0008101)
4          p3 =   -0.001516; % (-0.002791, -0.0002412)
5          p4 =   -0.001678; % (-0.003105, -0.0002511)
6          p5 =     0.01727; % (0.01044, 0.0241)
7          p6 =    -0.01682; % (-0.02712, -0.006512)
8          p7 =      -0.084; % (-0.09635, -0.07164)
9          p8 =      0.2422; % (0.2278, 0.2567)
10         p9 =      0.8146; % (0.8051, 0.8241)
11         p10 =     0.5977; % (0.5947, 0.6006)
12  %G-function
13  g30 = @(t) p1.*log10(t).^9 + p2.*log10(t).^8 + p3.*log10(t).^7 + p4.*log10(t).^6 + p5.*log10(t).^5 + p6.*log10(t).^4 + p7.*log10(t)
          .^3 + p8.*log10(t).^2 + p9.*log10(t) + p10;
14
15  T_end_year = 5; %simulation duration in year
16  T_end_seconds = T_end_year*365*24*60*60; %simulation duration in seconds
17
18  k_s = 2 ;                          %Thermal conductivity of soil
19  alpha_s = 8*10^(-7);               %Thermal diffusity of soil
20  r = 0.350;                         %Pile width [m]
21  AR = 30;                           %Aspect ratio
22  r_b = r*2/pi;                      %Equivalent pile radius [m]
23  Pile_L = AR*2*r_b ;                %Active pile length [m]
24  Pile_num = 12;                     %Pile number
25  Pile_L_tot = Pile_num*Pile_L;      %Total active pile length
26  Fo_factor = alpha_s/(r_b^2);
27  Fo_end = T_end_seconds*Fo_factor;
28  time_translate_end = round(20000+(Fo_end-1)); %An ending cell/number of cells in vector for simulating larger than 1 seconds
29  time_print = 14*24*60*60;              %Chosing how many days printing time for the pile wall temp at specific time
30  time_step = 24*60*60;                  %Chosing time step between all printing times
31
32  Fo_step = time_print*Fo_factor;
33  time_translate_step = round(Fo_factor*time_print);
34  N_realtime = round(T_end_seconds/time_print);
35  One_year = 365*24*60*60;
36  N_oneyear = round(One_year/time_print);
```

```matlab
37
38  T_0 = 8;                               %Undisturbed soil temperature
39  dT = 0 ;                               %The change of temperature
40  T_b = zeros(1,round(N_realtime)—1);    %Preallocating the wall temperature vector
41
42  C_time = 2232*3600;                    %93 days
43  H_time = One_year — C_time;
44  Hpeak = 5823.67; % [W] Heating peak demand %Hfreq =0.000481235; % [1/d]5.5698E—9 1/s, Heating sin function frequency
45  Cpeak = —810.27; %[W] Peak cooling demand %Cfreq =0.001407482; % [1/h]3.9097E—7 1/s, Cooling sin function frequency
46
47  t = (1:1:One_year);
48  HCD = zeros(1,N_oneyear);
49  counter = 0;
50
51  for i = 1:time_step:One_year            %Making the equivalent sinusodial curve with 1 day time stepping resolution
52      counter = counter + 1;
53      if i <= 2232*3600
54          HCD(counter) = Cpeak*sin(1*i/(2232*3600)*pi);
55      else
56          HCD(counter) = Hpeak*sin(1*(i—(2232*3600))/(6528*3600)*pi);
57      end
58  end
59  HCD_rep = repmat(HCD,1,T_end_year);                     %Repeating for the amount of simulation years
60  t_plot = zeros(1,round(N_realtime)—1);                  %Preallocting time plotting vector
61      count = 1;
62      dT = 0 ;
63      Test = zeros(1,round(N_realtime)—1);
64      celle = 1;
65  for n = time_print:time_print:T_end_seconds            %Calculating the temperature change for the spesified HCD and g—function
66      count = 1;
67      dT=0;
68      for i = time_step:time_step:n
69          if count == 1
70              dT = (((HCD_rep(count)/Pile_L_tot)/(2*pi*k_s))*g30(n*Fo_factor));
71              count = count + 1;
72          end
73          Fo = (n*Fo_factor) — i*Fo_factor + 0.001; %+0,001 because the Fo isn't defined for 0
74          dT = dT — ((((HCD_rep(count)—HCD_rep(count—1))/Pile_L_tot)/(2*pi*k_s))*g30(Fo));
75          count = count + 1;
76      end
77      T_b(celle) = T_0 + dT;
78      t_plot(celle) = n/(60*60*24*365);
79      Test(celle) = g30(Fo);
80      celle = celle + 1;
81  end
82  plot(t_plot, T_b)
83  legend('Tb: Insulated ground surface')
84  xlabel('Years')
85  ylabel('Temperature [degC]')
86  grid on
87  ylim([—4 10])
88  hold off
```

Appendix C

Specialization project report

Literature review and feasibility study for energy piles in Norway.

Olai Stensland Lillevold

Potential of geothermal energy piles in Norway

A feasibility study

Trondheim, June 2021

NTNU – Trondheim
Norwegian University of
Science and Technology

Preface

This report is a specialization project which forms the basis for the grade in the subject TBA4510 at NTNU. The scope of the subject is 7,5 ECTS credits and is a part of the MSc in Civil and Environmental Engineering with Geotechnical Engineering as a field of study. It was carried out during the spring semester of 2021.

Trondheim, 2021-06-18

Olai Stensland Lillevold

Acknowledgment

First of all I want to thank Professor Rao Martand Singh and Habibollah Sadeghi for all the help and the friendly meetings during the whole semester. The subject was quite unknown to me before this semester, but it was a pleasure to dive into the world of renewable resources. Due to the restriction related to the pandemic every meeting was done through Teams, so I hope there will be more possibilities to have some coffees together next year.

I also want to thank Jonas Henriksen from Centrum Pæle AS for being available for a meeting and willingly answering all my questions which helped a lot with the cost analysis.

I also want to thank my brother, Mathias, conversations with tips during the work with this project.

Last but not least I want to thank my girlfriend, Tonje, for always being supportive.

Olai Stensland Lillevold

Summary and Conclusions

A geothermal energy pile (GEP) is a renewable thermal energy source that can be used to heating and cooling of buildings. In Norway 33% of the total energy consumption goes to heating and cooling of buildings. For the households the share for heating and cooling is 78% where electricity is the main heating source at 80%. GEPs are a solution that can make the heating and cooling in buildings several times more efficient, both in Norway and many other countries. It can also contribute to cut unhealthy emissions of particulate matter from fuel wood in the winter. Waterborne heating systems are required for using energy piles. This type of heating system is not much used in Norway until now, but the use is increasing as the the awareness of its applicability to renewable heating sources also is increasing.

The cost analysis shows that the initial cost for a borehole heat exchanger (BHE) is much higher than for a GEP. The payback time for a GEP system for a detached residential house is calculated to be 18-20 years. The calculations have variables and assumptions that can influence the result and the result can thus vary. But the calculations does anyhow show that the energy piles can be, not just a non-emitting renewable source, but also economically favourable. For a larger system the payback time is usually lower at 2-10 years.

Geothermal energy is well known in Norway and the use is increasing. Norway is top five in geothermal energy use per capita and BHEs are the most used system with a share of 90%. GEPs are suitable for areas with thick layers of sedimentary deposits which are areas where the BHEs are more expensive to install. GEPs is thus a good alternative to the BHE in these areas where the building anyway will install pile foundation. The precast GEP have been proved feasible for the conditions in Denmark. It is further necessary to research how the energy piles will affect the soft ground conditions in Norway, which is already initiated in a project by SINTEF and NTNU.

Contents

Chapter 1

Introduction

As the calendar says 2021 we are well in the second year of the ongoing COVID-19 pandemic which have been responsible for a major threat to peoples health and a socioeconomic disruption in the world. Even though the pandemic caused a drawback of the greenhouse gas emissions, the energy demand is back to 2019 levels and the CO_2 are heading for the second ever largest increase, but there is positively also a large increase in the use of renewable technologies which are on track to set new records [1]. International Energy Agency (IEA) recently published the report "Net Zero by 2050" [2] where they present a path for policy makers for reaching net zero CO_2 emissions before 2050. IEA describes this path as *"consistent with efforts to limit the long-term increase in average global temperatures to 1.5 °C"* compared to preindustrial levels which is the goal of the Paris Agreement which signed by 197 Parties. Norway is bound by the Paris Agreement and by law through the climate change act § 4 [3] to be a low-emission society within 2050. The goal set is to reduce the green house gas emissions 80-90% from 1990 levels.

In the recent IEA-report the need for a fast transition from fossil fuel in the energy sector is stressed and there is a clear recommendation to boost innovation and clean investment in efficient renewable technology. Geothermal energy piles (GEP), that are the focus of the present study, use the renewable geothermal energy to heat and cool buildings and can be a piece in the puzzle of a sustainable future.

This report presents the possibilities of using energy piles in Norway. The purpose is to review the circumstances regarding the Norwegian energy consumption, governmental and climatic conditions and the current technology of energy piles to illuminate the possibilities of implementing this technology in Norway and the possible effects.

1.1 Background

Norway has got a large amount of renewable energy resources for electricity production. There is nevertheless need to make the energy consumption more efficient as the consumption and also the need for electricity are increasing. The energy consumption in Norway and the emissions is reviewed in chapter 2. Furthermore, a cost analysis is done between the initial cost of energy piles and conventional borehole heat exchanger (BHE) and the payback time compared to the use of electricity as heating source in chapter 3.

An energy pile is a vertical heat exchanger where you use the pile foundation of a structure to reach down in the ground. There are also other types of geostructures that can be used for this purpose. Pipes are added inside the piles and a heat pump exploits the stable temperatures and renewable thermal energy in the ground and in this way one can achieve heating of domestic hot water, spacial heating during the winter and cooling during summer. The use of energy geostructures in the world is increasing as well as the knowledge requirements on this type of GSHP system. The geothermal energy has been exploited in Norway since the middle of the 90's but energy geostructures such as energy piles have not been used in Norway until now. The stable temperatures over the ground depth gives a high coefficient of performance, and hence higher efficiency, compared to the air source heat pumps which exists in large numbers in Norway. Further introduction to other geothermal heat pump technologies will be presented in chapter 4 and description of the technical aspects of the energy piles in chapter 5.

1.1.1 Health effects

As a basis for the feasibility study of the energy piles in Norway some health issues that can be related to the usage of different energy sources are reviewed. Health effects related to indoor temperature and toxic gasses or particulate matter is found relevant for this paper.

In Norway there is a significant higher mortality rate for the elderly in the winter months compared to summer months [4]. This is a fact where the underlying causes for the deaths is complex and statisticians and scientist say that it is difficult to determine directly. They discuss how the indoor temperature is influencing these statistics. The tendency with higher mortality in the winter is larger for more southern European countries than Scandinavian countries. It is therefore discussed among scientists that the lower indoor temperature is a factor because of the

southern houses is built to handle warmer climate and not the cold winters [4]. It can therefore be a motivation to implement the heat exchanger technologies which can provide cooling in the summer as well heating in the winter with a higher efficiency and hence lower operation costs than direct electric heating. This could nevertheless have more effect on the mentioned southern European countries than for Norway as the indoor temperature seems to have more importance in this case [4].

The Norwegian Institute of Public health (NIPH) states that air pollution is the environmental problem that has the biggest health effects in Norway [5]. They have proposed to lower the limit values for particulate matter that are currently used and the most important measures to reduce the emissions are reducing the emissions from wood burning together with road traffic. The European Environment Agency (EEA) has estimated that there was 1 400 premature deaths in 2018 related to inhalable particulate matter ($PM_{2.5}$), where fuel wood is a big contributor to the emissions in Norway [6]. The numbers of premature deaths related to $PM_{2.5}$ in the EEA countries was estimated to be a total of 417 000 [6]. Hence has the Norwegian Environment Agency proposed in 2020 air quality standards for Norway related to particulate matter [7]. And introduces measures to reduce the emissions of particulate matter from fuel wood. Measures taken is motivation to buy stoves with higher efficiency.

1.1.2 Method

In this feasibility study it is done a selective literature review to answer whether the use of energy piles is possible in Norway.

To find the sources there has been done an extensive search through the databases "Engineering village" and "Google Scholar" with relevant searching word for the different topics. There has also been recommended research papers, standards and scientific literature from my academic supervisor Rao Martand Singh and Habibollah Sadeghi. There has additionally been used data from Statistics Norway, governmental and institutional reports as well as lecture notes from NTNU.

There has also been done an interview with with Jonas Henriksen in Centrum Pæle, which has especially helped with the cost analysis. The interview was done and recorded through Teams and the other communication has been through e-mail. It has also been done a telephone conversation with Kjell Ingar Helgemo from Rørlegger1 Tiller.

Chapter 2

Energy consumption in Norway

Norway is a country with high energy consumption and hence high energy intensity. In 2017 it was ranked as the fifth highest IEA member country in energy intensity calculated as total energy supply per capita [8]. The IEA states this not only comes from the fact that Norway has energy intensive industries as aluminium production but also that there are cold winters and extra energy used for heating buildings [8]. The present chapter will study the energy consumption in Norway. There will be a focus on the amount of energy and energy mix that goes into heating and cooling of buildings as thermal energy which is the type of energy harvested by energy piles.

2.1   Energy used for heating and cooling in Norway

Asplan Viak and Oslo Economics finished a report in 2020 for the Ministry of Petroleum and Energy which includes a review of the energy consumption used specifically for heating and cooling in Norway [9]. In this report they follow the requirements set by the EU energy efficiency directive. To calculate the energy specifically used to heat and cool buildings, they used statistical numbers from Statistics Norway combined with estimates based on expert interviews. The report only take into account the contribution of households, service and industry sectors because these are the most important sectors regarding the heating and cooling of buildings. The report present data which are relevant for this paper and the figures Figure 2.1 and Figure 2.2 are modified with the data from the NVE report.
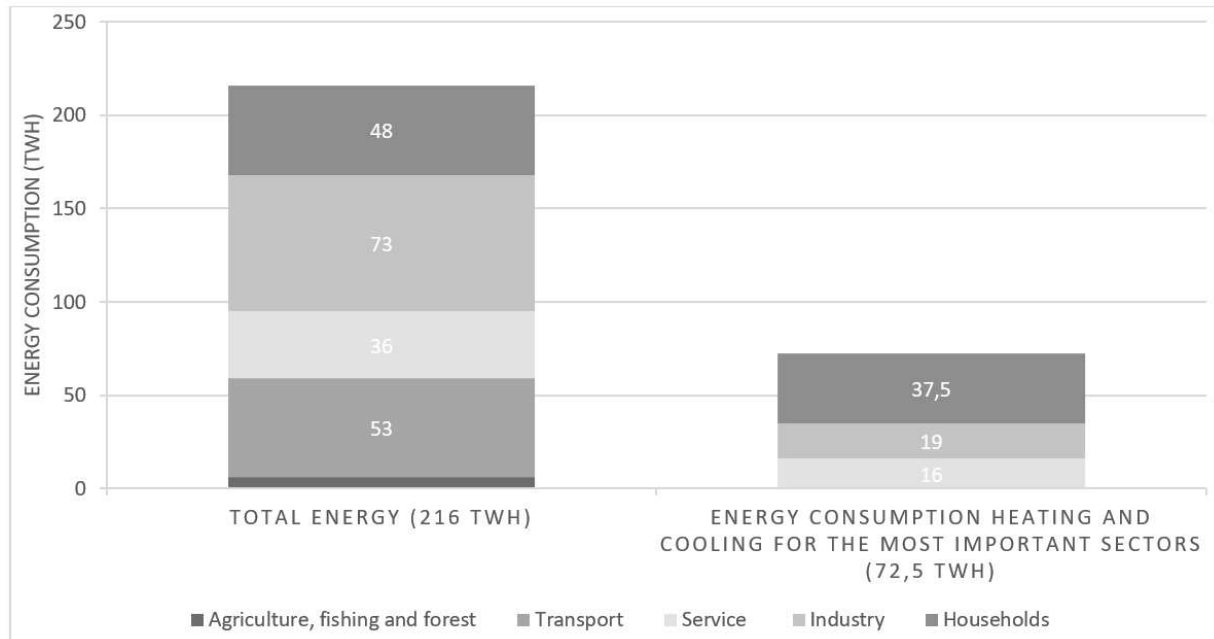
Figure 2.1: Total energy consumption and energy used for heating and cooling divided by sectors and for total energy used for heating and cooling. Modified from source: Oslo Economics, Asplan Viak and Statistics Norway

The total amount of energy used to heat and cool buildings in 2018 in Norway was estimated to be 72,5 TWh and more than 33% of the total energy consumption which was at 216 TWh [9]. As shown in the Figure 2.1 the amount of energy calculated for heating and cooling for households was at 37,5 TWh and distinctly higher than the other sectors. This gives a share of 78% of the total energy consumption for the service sector. For the industry the amount was 19 TWh and for service the amount was 16 TWh. This gives a 26% and 44% share, respectively, of total energy consumption for heating and cooling in the industry and service sector.

In governmental projections of the future energy consumption is it predicted that even though the population will increase, the energy consumption will decrease due to new and more efficient technology for heating [10].

2.1.1 Cooling in Norway

As the climate is cold in Norway there are much more energy used for heating than for spacial cooling. The NVE report estimates the share of cooling to be 3% of energy for heating and cooling [9]. The service sector is the greatest part with estimated 2,1 TWh in 2018

The market for for cooling is however estimated to increase. Apart from the global warm-

ing and increasing demand for heating and cooling, there are several sectors that require more spacial cooling than heating, which include but are not limited to new industries, data centers, shopping centers and warehouses. Also modern day architecture with glass facades for larger office buildings have more cooling needs [11].

2.2 Energy mix

Figure 2.2 shows the energy mix for the heating and cooling energy supply for total heating and cooling energy consumption and divided into energy sources for the different sector. The most important source is electricity for all the sectors with an 80% share of total energy to heating and cooling for household, for service it is 60%, industry it is 40% and the total was about 67% in 2018. In total the use of biofuel was about 12%, district heating approximately 8%, and oil products 6%. Oil products was from January 1st 2020 prohibited in use for building heating [12]. The share of oil used for heating will therefore already have declined from the data from 2018 and new heating technology will have taken over for heating buildings. The amount of renewable energy was 83%, 4% is from incineration to district heating and 13% is non-renewable sources.
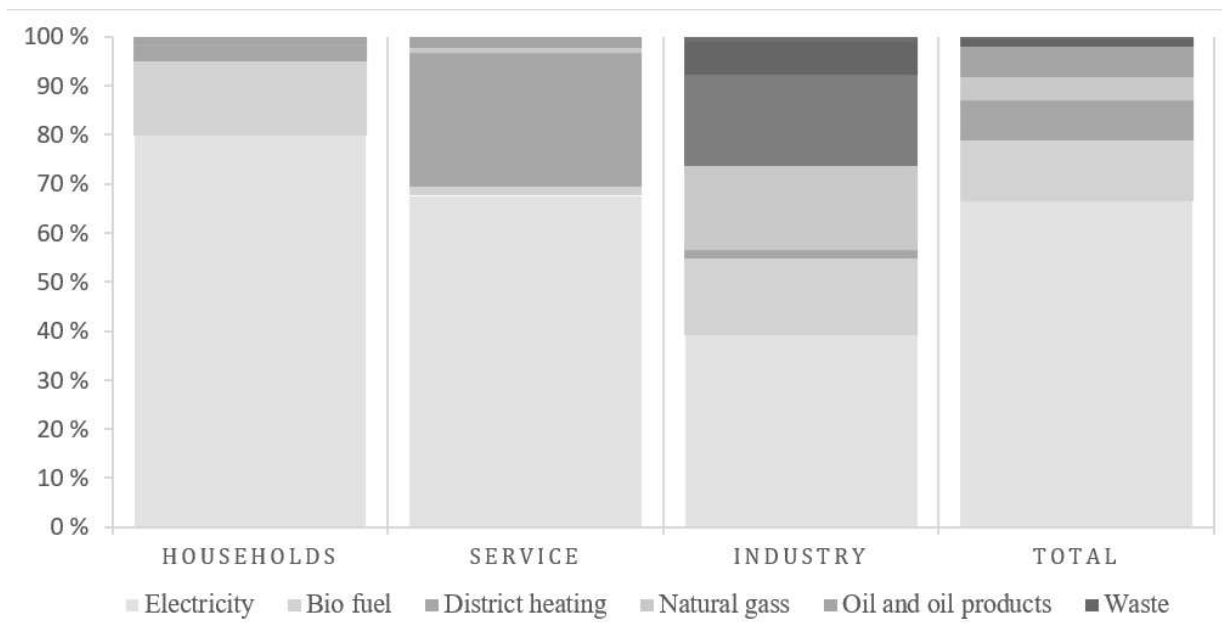

Figure 2.2: Energy supply divided into energy sources for the different sectors. Modified from source: Oslo Economics, Asplan Viak and Statistics Norway

The electricity production in Norway consists of 98% renewable energy. The topography of Norway is providing for a remarkable amount of hydropower with 90% in 2020 [13]. This also leads to very electricity prices in Norway which is dependent on the water recervoirs and hence the temperatures and rainfall. The second electricity source is wind power with more than 8% and less than 2% of the electricity production is based on thermal energy from fossil fuel and waste.

Taking the electricity export and import into account the share of renewable energy in Norway decreases to 94% but is still the highest share in Europe. Also with the import and export taken into account, the emissions related to electricity consumption in Norway is calculated to $17\ gCO_2e/kWh$ [14] in 2019. As a comparison, the European level related to electricity generation in 2019 was $275\ gCO_2e/kWh$ [15] and the world level was $475\ gCO_2e/kWh$ [16].

2.3   Fuel wood

As shown in Figure 2.2 the share of biofuel was about 15% for the households where the most significant part is fuel wood. In 2012 the amount of households using fuel wood as the main source for heating was estimated to be 12% [17]. In the last 30 years, the annual fuel wood consumption is as shown in Figure 2.3 between 5 and 8 TWh. In addition to this there are also an unregistered use with households in rural areas in which are self-sufficient of fuel wood. Most of the consumption is during winter to heat households.

Compared to other European countries the share of fuel wood consumption is lower in Norway, for instance, in Finland 25% of the heating energy is fuel wood, while the number is just 6% in Norway [18]! However, the contribution to the emissions of particulate matter in Norway is still high.

2.3.1   Emissions from wood burning

The emissions related to the fuel wood combustion is nitrogen oxides (NOx), carbon monoxide (CO) and particulate matter [5]. The particulate matter consists of organic compounds as for instance a high amount of polycyclic aromatic hydrocarbons.

When looking at particulate matter it is common to categorize in PM_{10} and $PM_{2.5}$ which is particulate matter with the size of less than 10 μm (inhalable) and 2,5 μm (fine inhalable). The
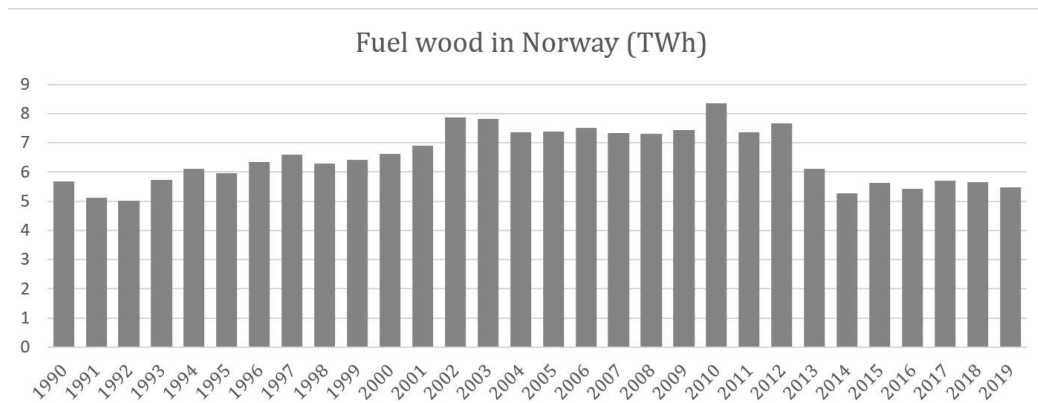
Figure 2.3: Fuel wood use in dwellings, cabins and holiday houses, by year. Source: Statistics Norway [19]

share of PM_{10} and $PM_{2.5}$ for the total emissions in Norway is more than 40% and 50%, respectively [20]. Because the emissions from fuel wood is several meters above ground level, human exposure is lower than for traffic-related PM, which is emitted from ground level [7]. A recent study researching the influence of wood combustion in four Nordic city shows that fuel wood has significant emissions in Oslo. This is due to the use of fuel wood combustion for heating larger apartment blocks [21].

The government recognized that there are health effects related to the PM from fuel wood and especially in smaller towns where fuel wood is the largest contributor to particulate matter emissions. Measures taken to reduce the emissions from fuel wood is especially motivating to buy new wood stoves with higher efficiency. There has been a transition towards newer and more efficient stoves. In 2019 almost 70% of the stoves in Norway was estimated to be new stoves produced after 1998 [17].

2.3.2 Health effects of wood smoke

Wood smoke gives as stated significant contribution to the $PM_{2.5}$. This is fine particles that can go all the way down in the air ducts and can accumulate in the lungs. $PM_{2.5}$ is associated with cardiovascular diseases and that causes adverse inflammatory symptoms for especially asthmatic children [22]. The $PM_{2.5}$ from fuel wood have a high content of polycyclic aromatic hydrocarbons (PAH) in wood smoke which can be carcinogenic [23].

A large and growing body in epidemiologic and toxicologic research emphasises the negative

health effects from exposure of wood smoke. Neaher et al. (2007) [24] state in their systematic literature review that "reducing woodsmoke emissions may be an effective means of lowering particle exposures" but concluded that there was "insufficient evidence at present to conclude that woodsmoke particles are significantly less or more damaging to health than general ambient fine particles".

Schwartz et al. (2020) reviewed studies on controlled human exposures to wood smoke. The authors discuss that several studies report significant health effects of various wood smoke exposures. They also states that the study of woodsmoke compared to other sources for fine particles is premature and more studies are needed [25].

However there are several new studies that shows that emissions from combustion of fuel wood is adverse and is not to be underestimated. A study from Australia concludes that PM with high wood smoke content was more inflammatory than just traffic related PM [26]. Another study states that emissions from fuel wood contributes to the underlying mechanisms leading
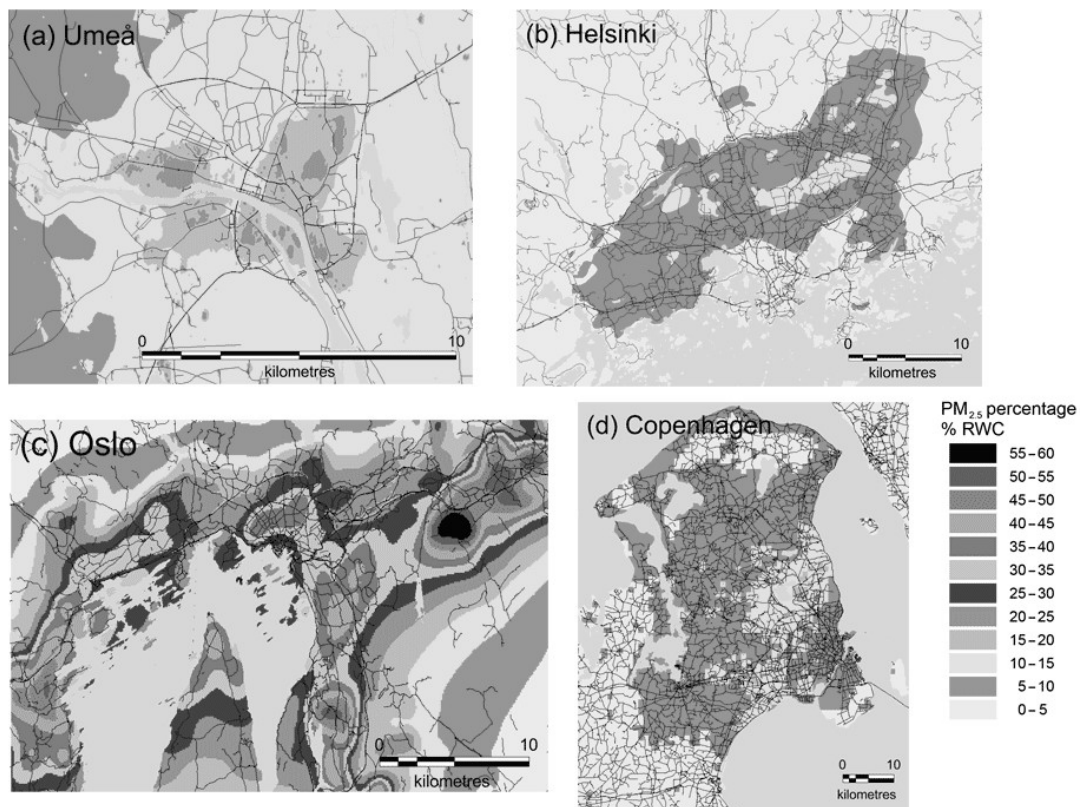

Figure 2.4: The percentage of fuel wood contribution to the PM2,5 fraction emmisions illustrated for the four Nordic countries Umeå, Helsinki, Oslo and Copenhagen. Source: Kukkonen et al. (2019) [21]

to pregnancy complications [27].

2.4   Heat pumps

The use of heat pumps in Norway has increased in the last years where air-to-air source heat pumps are installed. The credit for this can be prescribed to governmental measures with aid schemes through ENOVA. According to European Heat Pump Association (EHPA) Norway has the most heat pumps per capita in Europe. In 2020 the number of heat pumps was estimated to be 1,3 millions (REF). In 2018 it is estimated that 6 TWh electricity gave 16 TWh of heating energy from heating pumps [9]. The amount of thermal energy extracted from the ground using GSHP systems is estimated to be 3 TWh. The use is increasing and NVE estimates that the there is 8 TWh potential within 2030. The air source heat pumps are the most popular and about 90% of the stock consists of this type.

However, the large increase in usage shows that there is interest and willingness to use this heat pumps as a heating source in Norway especially with the help of incentive schemes. The cooling demand will also increase with warmer climate and nonetheless strict regulations on technical requirements for construction works and the energy efficiency.

2.5   District heating

District heating makes up 8% of the total energy for heating in buildings in Norway. The largest sector that benefits from this energy source the service industry, as presented in Figure 2.2. The price of district heating is in Norway bound by the law to not exceed the electricity prices and the cost should therefore reflect the electricity prices. The fuel sources used for district heating in Norway in 2020 consisted of about 51% energy from waste, 30% biofuel as pellets, 13% electricity, 3% waste heat and 3% fossil fuel [28]. The fossil fuel is contributing to the peak load and waste and biofuel is usually covering the base load. At the Heimdal production plant in Trondheim the amount of municipal waste is higher than the Norwegian average at about 70%. The BREEAM calculation for the plants of Statkraft showed a CO_2 emissions of 15-64 gCO_2e/kWh [29]. Compared to the CO_2 equivalent for the electricity in Norway this is a little higher. The technology has provided that for example schools and other buildings has been able to change from oil heating with the the more environmental friendly waste energy recovery. This heating

option is a a great way of recover also waste heat from industry as well as from the municipal waste.

An issue with the district heating is that the production system requires the waste to be burned throughout the summer. This produces a lot of waste heat which is not recovered but let out in the air. Geothermal solutions such as high temperature borehole thermal energy storage (HTBTES) can act as a thermal energy battery and therefore saves some of this waste heat.

2.6 Off-grid consumption i Norway

At Svalbard the main source of electricity production and district heating has been coal. In 2021, the Norwegian government stated that the coal power plant at Svalbard is going to be phased out within 2025 and that the government will include a plan for energy replacement at Svalbard in the 2022 government budget. This leads to the need of seeking new environmental friendly energy sources with lower cost for electricity and heating at Svalbard.

In 2018 a technical report for the Ministry of Petroleum and Energy looked upon different possible energy sources to replace the coal as energy source. LNG and pellets were the energy sources in which they wanted to consider in the further work to replace coal in the district heating system [30]. In the report they didn't analyse using geothermal energy due to the uncertainty in this technology and the economic aspect and that the high temperatures in the district heat system is difficult to meet with a geothermal heating system. Until now the heating demand has been covered only by district heating.

One point that is especially relevant for the topic of current project related to the use of pile foundations at Svalbard. Until now it has mainly consisted of steel and wooden piles that reach through the active layer, that is thawing during summer an freezes during winter, down to the permafrost. For avoiding settlements they need to cool down the ground during the summer to keep the soil frozen and the soil strength. By now the heat extracted from ground hasn't been exploited for heating. Is could therefore reasonable to consider energy piles as a possible energy source at Svalbard or other places with similar ground conditions. In Norway there exist a lot of leisure homes in which in many are remote and off grid. And they have good potential to use geothermal energy for heating and cooling.

Chapter 3

Cost analysis

While the GSHP systems are renewable heating sources that can for example mitigate the load on electricity grid and replace particulate matter emitting heating sources, they can also be economically favorable in the long run. Brandl (2006) [31] states that the energy pile systems have a payback period between 2-10 years depending on the ground properties, foundation system, building characteristics and energy prices. This is probably calculations for larger buildings and GSHP systems. It is also shown that the durability for this type of systems are good, they don't require any maintenance and according to Brandl (2016) [11] no long term failures had been observed.

3.1   Cost of different heating products

When comparing the different sources of thermal energy for buildings it is useful to have an outlook on the cost. The operating expenses are variable as presented in Table 3.1. The electricity prices are the average yearly prices for the last five years. The heat pump prices are dependent on the electricity prices and the COP of the system. For the fuel wood the cost varies depending on where you buy the wood , type of tree species and with the efficiency of the stove.

Table 3.1: Price in NOK/kWh for different heating sources. Electricity prices is from the last 5 years from Statistics Norway and the price for heat pump is based on the electricity price.

Heating source	Price [NOK/kWh]
Fuel wood	0,49 - 2,17 [32]
Electricity: total with grid rent and taxes	0,80 - 1,15 [19]
Heat pump: COP: 2.5-4	0,20 - 0,45

3.2   Example: Detached residential house

In this cost analysis it is assumed that the detached house has an energy consumption of 25 000 kWh per year. As presented in Figure 2.1 the amount of energy that goes to heating and cooling in Norwegian households is 78% which gives a total of 19 500 kWh for heating of the house. It is also assumed that the house is placed in an area with thick sedimentary layers so the house has already planned to use pile foundations. In this example we look at electricity compared to geothermal energy piles as energy sources.

When using electricity directly for heating the ratio for energy input to thermal output is usually less than 1 to 1. Using a heat pump the efficiency is higher and the same coefficient of performance (COP) is usually between 2 to 5. In this example the ground source heat pump is heating the domestic hot water as well as spacial heating.

Residential houses in Norway are heating dominated and there is minor cooling demand [33]. A GSHP system can however provide "free cooling" where it delivers comfort cooling at a very low cost. The "free cooling" is further described in chapter 5.

3.2.1   Initial cost

When using conventional ground source heat pumps there is an initial cost for drilling borehole which can cost between 40 000 and 100 000 NOK in Norway [34]. The cost is higher when boring is in sediments because there is need to seal the hole with a steel pipe. In this case we consider as mentioned a house that will be placed in an area with thick sedimentary layers and the cost is therefore assumed to be **100 000 NOK** in Table 3.2. This is also equivalent to the value derived using the calculation method from Ramstad [35] when assuming 35 meters to bedrock.

For energy piles there is assumed that the construction is going to install pile foundation independently of the energy part. The initial cost for the energy piles is thus consisting of the pipes within the piles and the cost of installation of the system. For one single pile at 18 meters the pipe cost is 1 690 NOK (Henriksen, J., Centrum Pæle AS, personal communication, 09.06.2021). The maximum length for the piles at Centrum Pæle AS is 18 meters long for the precast driven piles, but it will also be assumed that it is possible to derive 35 meters long driven piles that reaches down to the bedrock. In the calculation there will be assumed one single U-loop within the pile. The pipe cost for 1 pile at 35 meter length is hence 3 380 NOK. For the installation of the

Table 3.2: Inital costs for GEP system for a singel residential detached house compared to inital cost for BHE.

	Piles - 18 m	Piles - 35 m
Number of piles	5	10
Initial cost piles	34 300 NOK	25 850 NOK
Total inital cost for GEP	184 300 NOK	175 850 NOK
Savings compared to BHE	**- 65 700 NOK**	**- 74 150 NOK**

pipes to a manifold and heat pump 1 740 NOK/pile (Henriksen, J., Centrum Pæle AS, personal communication, 09.06.2021). This will be the same for both the different pile length. The cost for the energy piles is calculated from Danish to Norwegian kroners.

For a whole BHE system the total cost is typically a total of 250 000 NOK (K.I. Helgemo, Rør-legger1 Tiller, personal communication, 08.06.2021) with everything included: where borehole, waterborne heating and installation is the main expenses. We then assume an initial cost of 250 000 NOK for a BHE and take into account that the GEP system has an initial cost of 72 500 NOK lower than initial cost for BHE, as shown in Table 3.2. We then derive the initial cost for the whole system: **184 300 NOK** for 18 meters long piles and **175 850 NOK** for the 35 meters long piles.

3.2.2 Cost analysis

The net present value formula is as presented in Equation 3.1:

$$NPV = \sum \frac{R_t}{(1+i)^t} \tag{3.1}$$

Where R_t is the net cash inflow or outflow for year t, R_0 is here a negative value as the initial cost (-177 500 NOK in year 0), and $R_{1,2,3,..,n}$ is hence the yearly savings by using the energy piles compared to electricity as energy source. i is the interest rate, which is set to 4%. We then calculate for the inflation using the Equation 3.1. When using the electricity price 1,00 NOK/kWh and COP = 3,5 for the GEP system we get the savings:

$$R_t = (\text{cost el.}) - (\text{cost heat pump}) = 19500 \text{ kWh} * 1,00^{NOK}/_{kWh} - \frac{19500 \text{ kWh} * 1,00^{NOK}/_{kWh}}{3,5} = 13\,928 \text{ NOK}$$

The savings are highly dependent on the electricity price. In Norway the electricity price is very low compared to other European countries because of of the access to a large amount of hydropower.

For the detached house it is then calculated a payback time of **18 - 20 years** for a residential detached house. The input parameters are listed below in Table 3.3

Table 3.3: Input parameters in the cost analysis for a detached house.

Input	Value
Interest rate	4 %
El. price (avg. last 5 years is 0,975)	1,00 NOK/kWh
COP	3,5
Heating demand	19 500 kWh

3.3 Discussion on the cost analysis

The payback time of 18-20 years is a reasonable result for the GEP's when comparing this to other cost analysis looking at a residential house for instance a study looking at the cost effectiveness in Australia [36]. The lifetime of a heat pumps is usually expected to be 20 years. The GSHP system has however an expected lifetime longer than this, and if there was installed a heat pump with the price of 50 000 NOK in the 20th year, which is typical for a GSHP for a detached house (K.I. Helgemo, Rørlegger1 Tiller, personal communication, 08.06.2021), this cost will have a payback time at only 3 years and be payed back during the 23th year.

As mentioned the yearly savings are highly dependent on the electricity prices. For this calculation it is around 13 000 NOK a year, but with a different electricity price the saving can vary a lot from this. The higher the electricity price the more will be saved by using GSHP system.

It is necessary to mention that this cost analysis is based on many assumptions of different factors and the initial cost can vary. But this analysis can anyhow illustrate that the energy piles can be economically profitable.

If the current incentive schemes from ENOVA by installing a BHE and water borne system on total 20 000 NOK is considered in the analysis, the payback time goes down to 16-17 years.

Larger systems will have higher efficiency and reach a much lower payback time for the initial cost. A cost analysis for the Danish project with 14 larger buildings at Rosborg Ø had a payback time with just more than 4 years [37]. A similar analysis for a bigger system will most probably have a much shorter payback time.

The most used heat pump type in Norway, the air-to-air heat pump will usually take less than 3 year to save up the initial costs. But there are cost studies as [38] compared ASHP to a GSHP system favorable in the long run [38].

Also notable in this is that there is a large amount of the initial cost that is the water borne heating system. This system is anyhow also convenient when using other renewable resources as solar collectors which provides for free thermal energy.

Chapter 4

Ground source heat pumps

A heat pump systems is a technology in which provide efficient and environmental friendly heating and cooling. The heat pumps can be categorized into the two main categories: air source heat pumps (ASHP) and ground source heat pumps (GSHP) with also the the less used heat pump systems with waste heat, surface water and solar heat as sources [39]. The GSHP systems rely on the stable temperatures in the ground and gives a basis for a more efficient system compared to the air-source heat pump when the power output is maintained on the coldest day of the year.

Ramstad (2011) [40] estimated that all the building heat demand in Norway can be covered by GSHP systems. In this chapter there will be a introduction to different types of GSHP systems and more about the current usage in Norway.

4.1 Usage in world and Norway

There is a raised awareness of the use of geothermal energy and GSHPs in the world. Lund et al. (2020) [41] report the total annual geothermal energy use in 2019 to be 283.6 GWh which was a increase of more than 72% increase from 2015. There is further reported 88 countries that use geothermal energy, where China, USA, Sweden, Turkey and Japan that have the largest annual geothermal energy use. When looking at annual geothermal energy use per capita Iceland, Sweden, Finland, Norway and New Zealand score the highest.

The use of geothermal energy was introduced in Norway in the middle of 90's inspired by the neighbouring country Sweden [40] that had already knowledge with this technology for many

years.

The two main GSHP technologies in Norway is with the use of boreholes, which stands for about 90%, and the use of groundwater [40]. The average depth is 220 meters and the tendency is that deeper boreholes are being bored [42]. The last 12 years it have been installed yearly between 2000-4000 BHE's in Norway and by examine the graph of new boreholes and sold brine-to water heat pumps [42] it is fair to estimate the number of BHE to be 45 000 - 50 000. Compared to Sweden that has similar ground conditions this is low numbers as they had more than 300 000 installed GSHP systems related to residential houses in 2011 [40].

4.2 The technology

GSHP systems exploits the shallow geothermal energy which is defined as located in the uppermost 300 meters of the earth's crust. Below this is the deep earth heat. From Banks (2012) [43] the shallow ground source heat or the thermogeology is described as usually the solar energy that has been absorbed and stored in the subsurface, but it can also contain a component the the deep-earth heat flux. The ground isn't affected by the seasonal variations below 15 meters of the surface as in section 4.2. It is possible to use the geothermal energy directly or with a heat pump to lift the temperature. Because energy is low-entalpy and the temperatures are low there is need to lift the temperature with a heat pump when using it to heat buildings. The GSHP systems are divided into 3 main system components, and this is described for the energy pile in subsection 5.1.1. For the GSHP systems there are different configurations with two main types: open and closed loop.

4.2.1 Open-loop heat exchangers

This type of system exploits the stable temperatures in underground water by circulating the groundwater to a heat pump that extracts the heat. The water is usually goes back to the aquifer that it came from. This type of GSHP requires that there is a natural aquifer present that is highly permeable. Compared to closed loop system this is a more effective and cheaper system but can have more complications in the operation part due to clogging or bio-fouling.
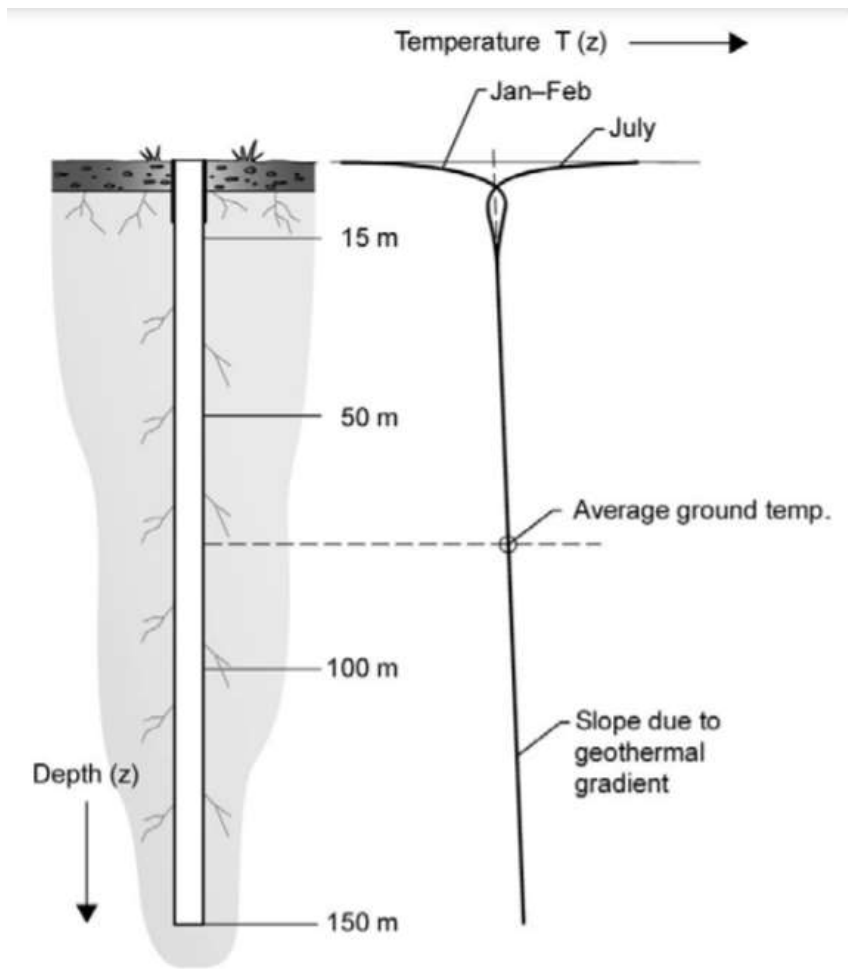
Figure 4.1: 15-20 meters below the surface the ground temperature is stable through the year. Source: Gehlin (2002) after Ericsson (1985) [44]

4.2.2 Closed-loop heat exchangers

In the closed loop system there is a heat carrier fluid that is circulated within a closed pipe to exploit the geothermal heat. There are three main types of the closed-loop ground source heat exchangers:

Shallow pipes which are placed at 1-3 meters below the surface. It can be placed as a serpentine, a coil or as baskets. This type requires more area than the other GSHP systems and you have to be careful when placing this so that you don't get complications and settlements due to freezing and thawing.

Borehole heat exchangers (BHE) where pipes are placed within vertical boreholes that usu-

ally go 50 to 250m deep.

The use of geostructures where the geostructures in the ground are exploited by placing the pipes within the structures. This includes tunnels, diaphragms, platforms and foundation piles. The energy pile system with design and influencing factors are further described in chapter 5.

There are a couple of values describing the efficiency heat pump system:

The coefficient of performance (COP) of a heat pump is defined by [31]:

$$COP = \frac{\text{energy output after heat pump [kW]}}{\text{energy input for operation [kW]}} \tag{4.1}$$

For the GSHP systems this mean that if a COP is for example 5, then 1 kWh of electricity goes to into the system to deliver 5kWh energy output to heat the building. Another important indicator in the efficiency on a heat pump system is the seasonal coefficient of performance (SCOP) which take into account the other energy consuming elements as the circulation pump and the system control:

$$SCOP = \frac{\text{usable energy output of the system [kWh]}}{\text{energy input for the system [kWh]}} \tag{4.2}$$

4.2.3 Energy storage

When having a large GSHP system it is possible to use this to store the energy either as for instance to cool a building or store waste heat. This is called underground thermal energy storage (UTES). When using the ground to cool the buildings in the summer it is a method to charge the ground so that a energy balance is ensured and the ground isn't for example gradually getting cooler and cooler in a heating dominated climate as Norway. This especially relevant for larger systems.

High temperature borehole thermal energy storage (HT BTES) is a new battery solution that is that can store thermal energy at higher temperature. New and sustainable battery solutions are important in the future energy consumption, especially when relying on intermittent electricity sources such as solar and wind power.

In Norway there has been established a HT BTES in Drammen with 100 boreholes at 50 meters depth, and the planning has started for a storage at Furuset in Oslo [45]. Trondheim municipality is considering using HT BTES to store waste heat from the local district heat plant [46]. It is also considered making Svalbard a seasonal energy storage in Longyearbyen at Svalbard [47].

4.3 Challenges in Norway

Ramstad (2011) [40] recognizes the main limitations due to the use of geothermal heat to be:

- Increase of cost with thicker sedimentary layers. This is because of the need to seal the borehole in the layer with loose material with a steel pipe casing. This makes that part 3-5 times more expensive per meter. It is estimated that 26% of the area of Norway is covered with depth to bedrock larger than 30m [40]. This is especially in valleys and places with marine deposits which is often densely populated as in parts of Oslo-area, Trøndelag, Jæren and Finnmark.

- There is not much available area in densely populated areas.

- The initial cost is high. There is a need for a fluid based heating system (secondary loop) in the building when using GSHP which is not so common in Norway and makes it more expensive to install in a building. The system can though be implemented in combination with solar collectors. The high electricity prices in the last years have been motivating to install a water borne heating system, and more people are choosing this in Norway than before when building new houses (K.I. Helgemo, Rør-legger1 Tiller, personal communication, 08.06.2021).

These problems have occurred when taking the the BHE and GHE into account. Geostructures and energy piles can possibly be solutions to the problems for the conventional GSHP systems. The area of use for energy piles are exactly in the areas with thick layer of sediments where there is need for pile foundations. The technology doesn't take up any more space than the already planned structure and also notable are the energy piles not in conflict with for example new underground tunnels and many BHE's as was a problem in 2017 during tunnelling for The Follo Line project [48]. The initial cost is also lower as described in chapter 3.

Chapter 5

Geothermal energy piles

The use of foundations as ground heat exchangers began in Austria and Switzerland in the 1980's. Energy piles specifically, was introduced in Austria in 1984. Brandl (2016) [11] describe Austria as a country with a pioneering role in using energy piles. The number of installed geothermal energy piles (GEP) in Austria from 1984 to 2004 was about 22 000 and in 2016 the number was almost 130 000 [11]. The use of GEP's has a high reported use in countries such as Switzerland, France UK and USA.

GEPs are geostructures that utilizes the shallow heat energy in the earth to heat and cool buildings. Energy geostructures are novel solutions that have gained a lot of interest and acceptance over the last two decades. This chapter will include a literature review that gathers research done on the subject. The present chapter is looking into the GEP subsections: GEP system, GEP design process, the factors that influence the performance of a GEP and short overview of different methods for analysing the performance of the piles.

5.1 Technology

When it comes to pile foundations there exist two main different pile types, which is bore or driven piles. The bore piles are pile which is made in-situ, also called cast-in-place, where the reinforcement cage is placed in the ground. The driven piles can be made of steel or concrete and is driven by either an impact or vibration hammer.

5.1.1 Energy pile system

GSHP systems is in the literature and Brandl (2006) [31] describes them as systems with 3 main units:

- **Primary loop**: For the energy piles this is consisting of the pipes that are integrated in the pile foundation by attaching them to the reinforcement. Heat carrier fluid (HCF) is circulated within the pipes. In colder climate the HCF is water and antifreeze fluid such as ethylene glycol.

- **Secondary loop**: Is consisting of the pipes and the system that delivers heating or cooling to the building.

- **Heat pump system:** Lifting the temperature of the heat extracted from the ground. The system is consisting of the components evaporator, condenser, compressor and expansion valve.

5.1.2 Heat transfer mechanisms

Heat transfer is always induced by temperature gradient where the heat goes from a warmer place to colder place. The different mechanisms, their importance in the soils and some formulas is presented underneath.

Heat conduction is recognized as the most predominant heat flow mechanism in soils [49] and it is also the only one that take place in concrete. This is the heat transfer due to contact between particles, and in the soil the particles are in close contact. Fourier's law gives the equation for the amount of heat that flows through an area in one dimension:

Heat convection Is the heat transfer induced by the differences in the temperature in a fluid. The hotter fluid have less density and will move upwards as it will be contarry for the colder fluid. Convection is neglicable in soils with grains smaller than sand [50].

Heat radiation is the heat transfer due to electromagnetic radiation. In soils with fine material the effect from this heat transfer mechanism is negligible [31]. The effect is anyhow larger with coarser grains.

Latent heat the energy that is required to change the aggregate state. This is for example when a liquid either vaporize or freeze or when a gas condensate or a solid material melts. Freezing and thawing should be avoided when this can have consequences and lead to settlements

for the buildings. The soil can be gradually colder in heating dominated areas using energy piles in colder areas, of this should thus be taken into account for the Norwegian conditions. Persisted frozen soil is however wanted for the soils and foundations at Svalbard, as mentioned in section 2.6.

5.1.3 Influencing factors

Ground water flow is influencing the the performance of the energy piles. With a higher ground water flow gradient the efficiency of the system will increase. The effective heat conductivity is often referred to as the thermal conductivity and the contribution from the ground water flow [35].

Ground initial temperature is also effecting the efficiency should be taken into account when designing the system. Down to 10-15 meters in the ground there are seasonal variations, but below this it is constant temperatures over the ground depth. GSHPA (2012) states that the undisturbed ground temperature shouldn't be below 2 °C [51]. This should by the designer demonstrate that this will not happen for operation the GSHP system for 100 years. This is so that the ground will not freeze. It is thus important that the freezing front must not reach down in the soil interface. The temperature should usually be between 4 and 30, but that UK have designed the system to have a temperature between -1°C and 30°C [52].

There are also factors as soil properties with soil type, geology and grain sizes as well as geography that gives the thermal properties [49]. It is thus necessary to take field test and soil samples to get these data when designing a GEP system.

5.1.4 Design

There exist standards and manuals for energy piles and GSHP systems in for example UK, Austria, Switzerland and Germany [53]. The simplified methods is often very limited and it is often recommended to use a software that can simulate the systems more accurately. The importance of a right designing for the system to obtain the highest performance is stressed in several studies [49].

There are different configurations of the pipes are researched and tried out on sites. The most common ones are the ones called single U-pipe, double U-pipe, W-pipe indirect double pipe and helix [53]. The heat extraction/rejection is dependent on the the configuration and

the pipe surface area within the pile, and the helix is one of the most effective. It is not always a desire to obtain the highest extraction rate, as for and the configuration should be carefully chosen for the specific case.

5.1.5 Thermo-hydro-mechanical behavior

As implied earlier there are many different physical factors that have to be taken into account when studying the performance of the energy piles.

- Firstly: The piles have to take the **mechanical load** from a construction

- Then there is the changes in temperature. Thus, the effects from the **thermal load** have to be determined. Heat extraction induces contraction and injection induces expansion [52].

- The temperature changes also induces convection and thus movement in the water present in the soil. Not only these effects but also the effect of the groundwater flow, which is referred to as advection, are **hydrodynamics** that will influence the performance of the energy piles.

It is different ways to analyse this behavior and it is possible to do numerical analysis, pile model test and full scale test.

5.2 Challenges and projects in Norway

There is initiated a project with a cooperation between the independent research center SIN-TEF and NTNU on the use of energy piles in Norway. The Norwegian climatic conditions and influence of the energy piles on the marine clay will be in focus.

5.3 Driven piles

It is typical in Norway with end-bearing piles where it is piled to rock contact when there is a thick soft top layer [54] [55]. The precast piles have to follow the requirements of the Norwegian standard NS3046. In Scandinavia the most frequent used pile for buildings are quadratic precast piles, with a side dimension of 270mm or 230mm, that are driven down in the ground. Below follows a literature review in the specifics for precast energy piles.

5.3.1   Installation

When it comes to the precast concrete piles there is two main different types: hollow and full piles. As mentioned it is the full precast that is used in Norway. The main advantage mentioned by Laloui and Loria (2019) [56] is that:

- Pipe fixing can be tailored an optimized to will.

- On-site climatic conditions isn't affecting the pile making.

The issues by precast piles is as well further mentioned:

- The whole pile doesn't necessarily reach down in the ground and it might have to be shortened.

- If it get damaged during driving, it can't be replaced.

5.3.2   Thermo-mechanical behavior

Studies in precast energy piles shows that the impact of the thermal cycles coupled with mechanical load will not lead to significant structural problems for pre-cast driven energy piles [57] [58] [59]. The respons from the tests shows heave during the heat-recovery cycles and settlement during the cooling-recovery cycles.

It have been done a lot of research on the bore piles in full scale, but not so much for driven piles yet. A full scale load test on driven piles with hollow PHC piles, with 15 m pile length, 0.4 m outside diameter, indicates that the driven piles behaves different than bored piles on thermal cycles and it is discussed that this can come from the densification of the soil surrounding the driven pile [60].

5.4   Thermal design

As mentioned there are different ways to analyse the performance of the energy piles and for designing the system with respect to the energy demand. The full scale field test yields good results but is an expensive method [60]. The thermal response test (TRT) is a method to determine the thermal resistance and performance. The numerical analysis can also yield high computational costs. Another method is a semi-empirical method using g-functions. The g-functions is: "dimensionless response factors that describe the change in temperature in the ground around a

heat exchanger with time as a result of an applied constant power" [61]. For the precast energy piles it has been shown that this yield very similar results as the 3D numerical model with lower computational cost [62] [63].

5.4.1 Free cooling

GSHP systems can be used to obtain cooling for the building with a very high efficiency and efficiency ratio at 24 to 36 have been noticed for precast energy piles [59].

The cooling is also a way to recharge the ground and store thermal energy during the summer. In a case study from Denmark, with 200 energy piles, the heating requirement of the building exceeded the free cooling. The asymmetric usage of the geothermal energy could imply a decrease in the ground temperatures. The temperature data from the HCF did however not go below 4.2 °C during the winter and the soil recovered to undisturbed conditions during the summer when heat demand is low and cooling demand is higher [64]. The study demonstrated that taking into account the energy demand is important in the design phase but also that there is a feasibility in heating dominated areas and Nordic conditions.

Bibliography

[1] IEA, "Global Energy Review 2021," tech. rep., Paris, 2021.

[2] IEA, "Net Zero by 2050," tech. rep., IEA, Paris, 2021.

[3] "Climate Change Act (LOV-2017-06-16-60)," 2017.

[4] T. Brenn and E. Ytterstad, "Dødelighet i Norge etter tid på året, ukedag og fødselsdato," *Tidsskrift for Den norske legeforening*, 6 2003.

[5] Miljødirektoratet and FHI, "Luftforurensning: Svevestøv," tech. rep., 2017.

[6] "Norway - Air pollution country fact sheet — European Environment Agency."

[7] Miljødirektoratet, "Forslag til reviderte grenseverdier for PM10 og PM2,5 Grenseverdier for svevestøv," tech. rep., Miljødirektoratet, Statens vegvesen Vegdirektoratet, Folkehelseinstituttet og Meteorologisk institutt, 2020.

[8] E. Policies of IEA Countries Norway, "ENERGY POLICIES OF IEA COUNTRIES Norway 2017 Review Together Secure Sustainable," tech. rep.

[9] "Kartlegging og vurdering av potensial for effektivisering av oppvarming og kjøling i Norge - Asplan Viak/ Oslo economics," tech. rep., NVE, 2019.

[10] D. Spilde, K. Lien, I. Magnussen, and T. Ericson, *Energibruk i Norge mot 2035*.

[11] H. Brandl, "Geothermal Geotechnics for Urban Undergrounds," in *Procedia Engineering*, vol. 165, pp. 747–764, Elsevier Ltd, 2016.

[12] "Forskrift om forbud mot bruk av mineralolje til oppvarming av bygninger (FOR-2018-06-28-1060) - Lovdata," 2020.

[13] Ministry of Petroleum and Energy, "Electricity production - Energifakta Norge," 2021.

[14] NVE, "Hvor kommer strømmen fra?," 2020.

[15] "Greenhouse gas emission intensity of electricity generation in Europe — European Environment Agency."

[16] I. Energy Agency, "The IEA examines the full spectrum of energy issues including oil," tech. rep., 2018.

[17] P. G. Røhnebæk, "Vedforbruket redusert med en tredel siden 2010 - SSB," 2021.

[18] Whelminger, "Archive:Wood as a source of energy - Statistics Explained," 12 2016.

[19] "09007: Kraftpris, nettleie og avgifter for husholdninger 2012 - 2020. Statistics Norway," 2020.

[20] "08942: Svevestøv, organiske miljøgifter, etter utslippskilde, energiprodukt og komponent 1990 - 2019. Statistics Norway," 2019.

[21] J. Kukkonen, S. López-Aparicio, D. Segersson, C. Geels, L. Kangas, ..., and J. Brandt, "The influence of residential wood combustion on the concentrations of PM2.5 in four Nordic cities," *Atmospheric Chemistry and Physics*, vol. 20, pp. 4333–4365, 4 2020.

[22] R. W. Allen, T. Mar, J. Koenig, L. J. Liu, T. Gould, C. Simpson, and T. Larson, "Changes in lung function and airway inflammation among asthmatic children residing in a woodsmoke-impacted urban area," *Inhalation Toxicology*, vol. 20, pp. 423–433, 2 2008.

[23] B. Armstrong, E. Hutchinson, J. Unwin, and T. Fletcher, "Lung cancer risk after exposure to polycyclic aromatic hydrocarbons: A review and meta-analysis," 2004.

[24] L. P. Naeher, M. Brauer, M. Lipsett, J. T. Zelikoff, C. D. Simpson, J. Q. Koenig, and K. R. Smith, "Woodsmoke health effects: A review," 1 2007.

[25] C. Schwartz, A. K. Bølling, and C. Carlsten, "Controlled human exposures to wood smoke: A synthesis of the evidence," 10 2020.

[26] B. Wang, H. Chen, D. Xenaki, J. Liao, C. Cowie, and B. G. Oliver, "Differential inflammatory and toxic effects in-vitro of wood smoke and traffic-related particulate matter from Sydney, Australia," *Chemosphere*, vol. 272, p. 129616, 6 2021.

[27] L. Erlandsson, R. Lindgren, Nääv, A. M. Krais, B. Strandberg, T. Lundh, ..., and E. Malmqvist, "Exposure to wood smoke particles leads to inflammation, disrupted proliferation and damage to cellular structures in a human first trimester trophoblast cell line," *Environmental Pollution*, vol. 264, p. 114790, 9 2020.

[28] "04730: Consumption of fuel used for gross production of district heating (GWh), by type of energy, contents and year. Statbank Norway."

[29] Statkraft, "Lokale miljødata - BREEAM," 2020.

[30] "Utarbeidet for Olje-og energidepartementet juni, 2018 Alternativer for framtidig energiforsyning på Svalbard," tech. rep.

[31] H. Brandl, "Energy foundations and other thermo-active ground structures," *Geotechnique*, vol. 56, pp. 81–122, 3 2006.

[32] P. Storm-Mathisen, "Er ved egentlig billigst?."

[33] J. Stene and O. Smedegård, "Hensiktsmessige varme- og kjøleløsninger i bygninger," tech. rep., 2013.

[34] "Bergvarme | Varmepumpe-Pris.no."

[35] R. K. Ramstad, "Energibrønner som varmekilde forvarmepumper - Lecture notes," 2017.

[36] Q. Lu, G. A. Narsilio, G. R. Aditya, and I. W. Johnston, "Economic analysis of vertical ground source heat pump systems in Melbourne," *Energy*, vol. 125, pp. 107–117, 4 2017.

[37] "Vedvarende, bygningsintegreret varme- og køleforsyning til fremtidens resiliente byer — UC Viden - Professionshøjskolernes Videndatabase."

[38] G. A. Narsilio, "Cost Effectiveness of Energy Piles in Residential Dwellings in Australia," *Current Trends in Civil & Structural Engineering*, vol. 3, 7 2019.

[39] I. Staffell, D. Brett, N. Brandon, and A. Hawkes, "A review of domestic heat pumps,"

[40] R. K. Ramstad and A. Viak, "Grunnvarme i Norge - kartlegging av økonomisk potensial," tech. rep., 2011.

[41] J. W. Lund and A. N. Toth, "Direct Utilization of Geothermal Energy 2020 Worldwide Review," tech. rep.

[42] K. H. Kvalsvik, K. Midttømme, and R. K. Ramstad, "Geothermal Energy Use, Country Update for Norway," tech. rep., 2019.

[43] D. Banks, *An Introduction to Thermogeology: Ground Source Heating and Cooling.* 2 ed., 2012.

[44] S. Gehlin, "Thermal Response Test Method Development and Evaluation," tech. rep., 2002.

[45] R. K. Ramstad, "Lecture notes TGB4855," 2021.

[46] "Termos-metode kan varme tusener på Nyhavna, www.trondheim2030.no," 2020.

[47] "Vil bygge gigantisk geotermos på Svalbard - ww.tu.no," 2021.

[48] M. E. Kvam, *Tunneler og energibrønner.* PhD thesis, 2018.

[49] A. K. Sani, R. M. Singh, T. Amis, and I. Cavarretta, "A review on the performance of geothermal energy pile foundation, its design process and applications," *Renewable and Sustainable Energy Reviews*, vol. 106, no. July 2018, pp. 54–78, 2019.

[50] O. T. Farouki, "Thermal properties of soils ," tech. rep., 1981.

[51] "Thermal Pile Design, Installation & Materials Standards," 2012.

[52] H. Peron, C. Knellwolf, and L. Laloui, "A Method for the Geotechnical Design of Heat Exchanger Piles," pp. 470–479, American Society of Civil Engineers (ASCE), 3 2011.

[53] J. Fadejev, R. Simson, J. Kurnitski, and F. Haghighat, "A review on energy piles design, sizing and modelling," *Energy*, vol. 122, pp. 390–407, 2017.

[54] A. Oelnes, "Betongpeler," in *Lecture during NGF course April,* (Sarpsborg), 2001.

[55] "Peleveiledningen. From the Norwegian piling committee," in *Norwegian Geotechnical Society*, 2012.

[56] L. Laloui and A. F. R. Loria, *Analysis and Design of Energy Geostructures.* Elsevier, 2020.

[57] M. Alberdi-Pagola, S. Madsen, R. Jensen, and S. Poulsen, "Numerical Investigation on the Thermo-mechanical Behavior of a Quadratic Cross Section Pile Heat Exchanger," Oklahoma State University Library, 2 2017.

[58] C. De Santiago, F. Pardo De Santayana, M. De Groot, J. Urchueguía, B. Badenes, T. Magraner, J. L. Arcos, and F. Martín, "Thermo-mechanical behavior of a thermo-active precast pile," tech. rep., 2016.

[59] S. E. Poulsen, M. Alberdi-Pagola, D. Cerra, and A. Magrini, "An experimental and numerical case study of passive building cooling with foundation pile heat exchangers in Denmark," *Energies*, vol. 12, no. 14, 2019.

[60] G. Jiang, C. Lin, D. Shao, M. Huang, H. Lu, G. Chen, and C. Zong, "Thermo-mechanical behavior of driven energy piles from full-scale load tests," *Energy and Buildings*, vol. 233, p. 110668, 2 2020.

[61] Eskilson and P, "Thermal analysis of heat extraction boreholes," 1987.

[62] M. Alberdi-Pagola, S. E. Poulsen, R. L. Jensen, and S. Madsen, "Thermal design method for multiple precast energy piles," *Geothermics*, vol. 78, pp. 201–210, 3 2019.

[63] M. Alberdi-Pagola, S. E. Poulsen, R. L. Jensen, and S. Madsen, "A case study of the sizing and optimisation of an energy pile foundation (Rosborg, Denmark)," *Renewable Energy*, vol. 147, pp. 2724–2735, 3 2018.

[64] M. Alberdi-Pagola, R. Jensen, and S. Poulsen, "A performance case study of energy pile foundation at Rosborg Gymnasium (Denmark)," 5 2016.